Liu *et al. Microstructures* 2023;3:2023020
DOI: 10.20517/microstructures.2023.02

Microstructures

Review

Open Access

Check for updates

A review on pitting corrosion and environmentally assisted cracking on duplex stainless steel

Menghao Liu[1], Cuiwei Du[1], Zhiyong Liu[1], Li Wang[1], Rui Zhong[2], Xiaojie Cheng[1], Jiawei Ao[1], Teng Duan[1], Yuetong Zhu[1], Xiaogang Li[1]

[1]Institute for Advanced Material and Technology, University of Science and Technology Beijing, Beijing 100083, China.
[2]Collaborative Innovation Center of Steel Technology, University of Science and Technology Beijing, Beijing 100083, China.

Correspondence to: Prof. Cuiwei Du, Institute for Advanced Material and Technology, University of Science and Technology Beijing, Beijing 100083, China. E-mail: dcw@ustb.edu.cn

How to cite this article: Liu M, Du C, Liu Z, Wang L, Zhong R, Cheng X, Ao J, Duan T, Zhu Y, Li X. A review on pitting corrosion and environmentally assisted cracking on duplex stainless steel. *Microstructures* 2023;3:2023020. https://dx.doi.org/10.20517/microstructures.2023.02

Received: 16 Jan 2023 **First Decision:** 3 Mar 2023 **Revised:** 7 Mar 2023 **Accepted:** 28 Mar 2023 **Published:** 18 Apr 2023

Academic Editor: Xiaozhou Liao **Copy Editor:** Fangling Lan **Production Editor:** Fangling Lan

Abstract

Duplex stainless steel is widely used in the petrochemical, maritime, and food industries. However, duplex stainless steel has the problem of corrosion failures during use. This topic has not been comprehensively and academically reviewed. These factors motivate the authors to review the developments in the corrosion research of duplex stainless steel. The review found that the primary reasons for the failure of duplex stainless steels are pitting corrosion and chloride-induced stress corrosion cracking. After being submerged in water, the evolution of the passive film on the duplex stainless steel can be loosely classified into three stages: nucleation, rapid growth, and stable growth stages. Instead of dramatic rupture, the passive film rupture process is a continuous metal oxidation process. Environmental factors scarcely affect the double-layer structure of the passive film, but they affect the film's overall thickness, oxide ratio, and defect concentration. The six mechanisms of alloying elements on pitting corrosion are summarized as stabilization, ineffective, soluble precipitates, soluble inclusions, insoluble inclusions, and wrapping mechanisms. In environments containing chlorides, ferrite undergoes pitting corrosion more easily than austenite. However, the pitting corrosion resistance reverses when sufficiently large deformation is used. The mechanisms of pitting corrosion induced by precipitates include the Cr-depletion, microgalvanic, and high-stress field theories. Chloride-induced cracks always initiate in the corrosion pits and blunt when encountering austenite. Phase boundaries are both strong hydrogen traps and rapid hydrogen diffusion pathways during hydrogen-induced stress cracking.

Keywords: Duplex stainless steel, passive film, pitting corrosion, stress corrosion cracking, hydrogen embrittlement

INTRODUCTION

Duplex stainless steel has gained wide acceptance in the papermaking, petroleum, food processing, and marine industries as a material of choice for systems, structures, and components due to the combination of high strength, good toughness and excellent corrosion resistance. This is attributed to the synergistic collaboration between the ferrite and austenite phases. Duplex stainless steels are more resistant to intergranular corrosion than austenitic stainless steels, because the combination of the austenite-ferrite boundary and the ferrite phase enables the precipitation of chromium carbides without severely depleting chromium at the phase boundaries[1]. The high solubility and slow diffusion rate of hydrogen in the austenite phase of duplex stainless steel make it more difficult for hydrogen to diffuse, distinguishing duplex stainless steel from ferritic stainless steel[2].

However, as application fields have expanded, it has become clear that duplex stainless steel suffers from corrosion problems. In acidic environments, duplex stainless steels suffer from severe selective corrosion of the austenite phase[3]. In the moist H_2S environment, duplex stainless steel faces the risk of sulfide stress cracking[4]. From 2000 to 2022, several failures have been documented in journals and conferences, including *CORROSION*, *Engineering Failure Analysis*, and *Journal of Failure Analysis and Prevention*, as illustrated in Figure 1[3-8] and presented in the supplemental material [Supplementary Table 1]. Environmentally-assisted cracking (EAC), which includes hydrogen-induced stress cracking (4.55%), sulfide stress cracking (18.18%), and chloride-induced stress corrosion cracking (27.27%), accounted for 50% of the failures. Pitting corrosion-induced failures accounted for 27.27% of the failures. Additionally, both microbially-induced corrosion (MIC) and selective corrosion caused 9.09% of the failures. Crevice corrosion was responsible for 4.55% of the failures. The majority of the failures were attributed to pitting corrosion and EAC. To ensure the safety of duplex stainless steel in industrial practice, it is imperative to undertake rigorous academic investigations into these issues.

Nevertheless, current review articles mainly emphasize the production processes, such as hot working, machinability and weldments[9-14]. Only a few reviews have discussed the service processes of duplex stainless steel. de Farias Azevedo *et al.* summarized some failures of duplex stainless steels, which focused on the failures induced by improper heat treatment[15]. However, the report is deficient in academic studies concerning failures related to corrosion. Salthalaand highlighted failures in the oil and gas industry, which focus on practical advice[16]. Cassagne and Elhoud reviewed the hydrogen embrittlement of duplex stainless steels[17,18]. Since their reviews were conducted ten years ago, new findings should be added, such as the recent research on the distribution of hydrogen in the two phases and at phase boundaries. Pan performed a mini-review summarizing research on passive films using synchrotron-based analyses[19]. Han *et al.* reviewed the function of the alloying elements in duplex stainless steel, which shed little on the corrosion behavior[20]. In response to the demands of industry and the paucity of comprehensive reviews dedicated to corrosion related to practical applications, this review was undertaken to fill this knowledge gap.

This article aims to review the recent academic progress on the pitting corrosion and EAC of duplex stainless steel, which are the most common causes of failures. Because the formation and degradation of the passive film are the basis for understanding the corrosion of duplex stainless steel, this review first introduces the research on passive films from the perspective of the formation process and degradation process of the passive film. Subsequently, the progress on pitting corrosion research is reviewed and summarized from the perspectives of alloying elements and microstructures. Various distinct pitting

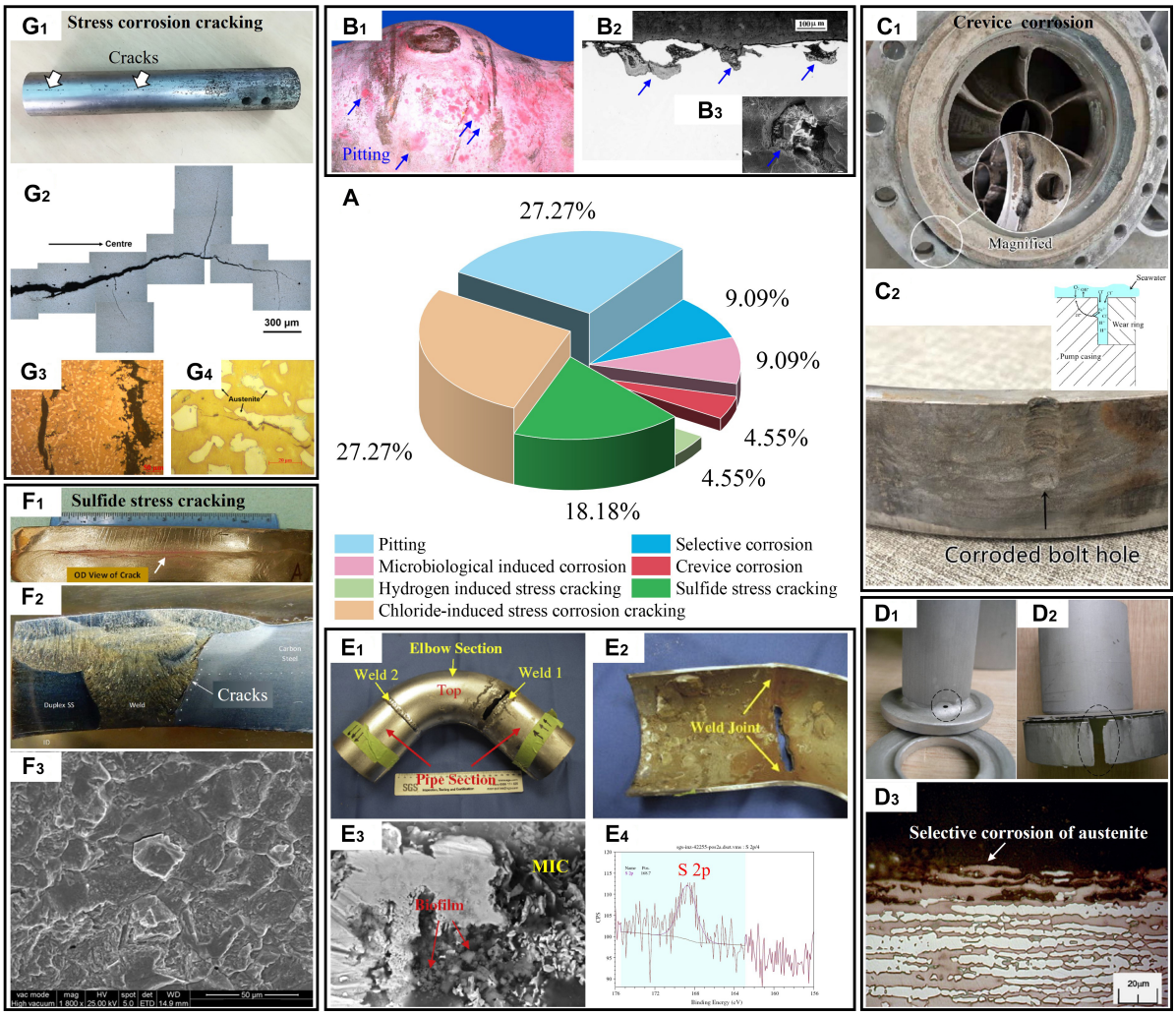

Figure 1. Environment-related failure statistics and typical cases of duplex stainless steel from 2000 to 2022. (A) Causes of failures and their proportions and (B) Failure caused by pitting corrosion (Reproduced with permission[5]. Copyright 2009, Elsevier). (B_1) Pitting corrosion was observed at the weld during the industrial inspection, (B_2) cross-sectional morphology of pitting corrosion, and (B_3) enlarged morphology of a pitted area. (C) Failure caused by crevice corrosion[6]. (Open access). (C_1) The failure point was located at the joint and (C_2) corrosion occurred along the contact area between the workpieces. A schematic diagram of the crevice corrosion mechanism is shown on the top right. (D) A failure caused by selective corrosion. (Reproduced with permission[3]. Copyright 2015, Elsevier). (D_1 and D_2) Corrosion caused perforation, and (D_3) the austenite phase was selectively corroded. (E) Failure caused by microbially-induced corrosion (MIC). (Reproduced with permission[7]. Copyright 2014, Elsevier). (E_1) Corrosion caused perforation at the weld, (E_2) the internal tube was covered with corrosion products, (E_3) biofilm was observed in the corrosion products, and (E_4) corrosion products containing sulfur element (S), indicating that corrosion was caused by sulfate-reducing bacteria (SRB) and sulfur-oxidizing bacteria (SOB). (F) Failure caused by sulfide stress cracking[8]. (Open access). (F_1) Cracking occurred near the weld/matrix interface, (F_2) cracks propagated along the side of the fusion line, and (F_3) fracture exhibited typical cleavage features. (G) Failure due to stress corrosion cracking. (Reproduced with permission[4]. Copyright 2018, Elsevier). (G_1) Cracks were visible along the length of the pipe and there was significant pitting corrosion on the pipe surface, (G_2) cross-sectional cracks with obvious dendritic bifurcations, (G_3) at the crack-propagating regions, the cracks propagated within both ferrite and austenite and (G_4) at crack-tip regions, the cracks expanded preferentially in ferrite.

corrosion mechanisms proposed in the literature to date are summarized in this section. Subsequently, the most recent studies on EAC are reviewed, and the EAC mechanisms and the most recent experimental findings are outlined. Finally, prospects for further corrosion research on duplex stainless steels are proposed.

PASSIVE FILM

Stainless steel is more corrosion-resistant than carbon steel in many applications because a dense film is formed on the surface, shielding the matrix from corrosive media. The passive film of duplex stainless steels consists of nanocrystals, hydroxides, and mixed oxides[19]. The two phases of duplex stainless steels have a gradient in their chemical composition, raising the question of whether or not their film-formation and film-degradation processes differ in any way. These issues have recently been addressed in passive film research on duplex stainless steels. This section introduces the research progress from the perspective of film formation and film degradation.

Formation of the passive film

Formation process of passive film

Chromium and molybdenum in duplex stainless steels are enriched in the ferrite phase, whereas the content of nickel and molybdenum in austenite is higher [Table 1][21-23]. The composition difference would lead to the formation difference of passive film. Overall, there is a lack of research in this area, and few studies have been published. Some scholars believe that the final passive film is dependent on the oxidation potential and ion solubility of the individual elements. Therefore, they extrapolated from the electrochemical behavior of pure metals in the environment to the composition of the passive film. Yao *et al.* predicted the passive film composition of 2,205 duplex stainless steel at different potentials by comparing the polarization curves of pure iron and pure chromium[24]. The composition of the passive film in duplex stainless steel can be readily determined using this method, which is interesting to consider. However, this view assumes that there is no interaction between the interphase passive films. This assumption might be debatable at the phase boundaries.

Another approach is to observe the passive process *in situ*. The evolution of passive films over 600 min was characterized using electrochemical atomic force microscopy (EC-AFM)[25]. Oxide particles were formed separately during the first 100 min, after which they completely covered the surface [Figure 2][25]. However, the low time resolution of EC-AFM, as compared to the rapid formation of passive films, is a drawback of this technology. Passive films form within seconds of exposure. Hence, the above study could not adequately capture the initial process of passive film formation. In recent years, researchers have also attempted to capture the formation process *in situ* at the nanometric scale using high-resolution techniques. This has yielded favorable results for the investigation of austenitic stainless steel[26,27]. Using scanning tunneling microscopes, the local oxidation of chromium was observed[26]. Therefore, a local inhomogeneity is generated once the passive film is formed. However, these studies focused on austenitic stainless steel. Further studies on the coupling process between nitrogen element and chromium element, the formation process at grain boundaries and phase boundaries, and the differences in passive film formation between ferrite and austenite from on the nanometric scale are promising for unveiling the mechanism responsible for the high corrosion resistance of duplex stainless steel. Furthermore, from a cross-sectional perspective, it is currently unknown how the passive film grows longitudinally. There are insufficient data to determine whether the oxidation is internal or external.

The study of the *in situ* passive film growth process in liquid may be another research direction because the current research is performed under electrochemical polarization conditions or in air. The state of the passive film in air differs from that in a real liquid environment. CrOOH in the passive film, which is one of the main components of the passive film in air, may react with water into other substances once it is immersed in the NaCl solution[28].

Table 1. The chemical composition of the matrix and the phases (wt.%)

Material	Phase	Cr	Mo	Ni	Mn	Ref.
UNS S32101	Total	21.69	0.36	1.56	4.92	[21]
	α	22.643	0.435	1.276	4.710	
	γ	20.735	0.280	1.857	5.247	
UNS S32205	Total	22.44	3.24	5.99	1.38	[22]
	α	23.604	4.216	5.003	1.300	
	γ	21.501	2.540	7.231	1.493	
UNS S32750	Total	24.48	4.00	6.36	0.54	[23]
	α	27.428	4.693	5.807	0.450	
	γ	24.299	3.08989	8.810	0.495	

(Reproduced with permission[21].Copyright 2019 Elsevier) (Reproduced with permission[22].Copyright 2014, Elsevier) (Reproduced with permission[23].Copyright 2015, Elsevier).

Composition and structure of the passive film

Research on passive films has focused on studying the composition and structural differences between the ferrite and austenite phases of the passive film, as shown in Figure 3[29,30]. There is a difference in the chemical composition of the passive film formed between ferrite and austenite. The contents of chromium, molybdenum and tungsten are higher in the ferritic passive film than that in the austenitic passive film. The nitrogen and nickel contents in the austenitic passive film are higher than those in the ferritic passive film[29-32]. Nickel is chemically stable and does not form oxides, which is mainly concentrated at the film/matrix interface[24]. However, both passive films are structurally composed of an outer film rich in iron and molybdenum and an inner film rich in chromium, with almost the same thickness and structure[30,32]. Other literature has shown that the passive film conductivity of the austenite phase is higher than that of the ferrite phase[33]. The crystal orientation may influence the passive film, which was identified by synchrotron hard X-ray photoemission electron microscopy (HAXPEEM)[29]. The (111) ferrite grains exhibit the lowest chromium content among the different orientations of ferrite, while the Cr_2O_3 content in the (111) ferrite grains is higher than that in the (111) austenite grain[29].

Environmental response of passive film

Environmental factors that cause corrosion failures of duplex stainless steels include pressure, temperature, sulfide, sodium hydroxide, chloride ions, vibration, and applied potentials[17]. Therefore, the effects of these factors on the composition and structure are discussed in the subsequent sections. Upon immersion in water, the structure and composition of the passive film change [Figure 4A and B][26,28]. Once immersed, the surface strain of the passive film decreases and relaxation occurs[28]. Furthermore, the content of CrOOH in the passive film decreases upon immersion in water, and when immersed in a 0.1 M NaCl solution, CrOOH vanishes [Figure 4B][28].

Based on the thermodynamic Pourbaix diagram, increasing the temperature narrows the region of metallic Fe, Cr, and Ni. Cr_2O_3 and Cr $(OH)_3$ are transformed into $FeCr_2O_4$, CrOOH, and $HCrO_2$[34]. From the perspective of the corrosion process, the temperature thickens the passive film and increases the point defects density in the passive film by analyzing the electrochemical data [Figure 4C][35]. When the temperature exceeds 40 °C, the electrochemical impendence spectra (EIS) show two-time constants, indicating that the structure changed[36]. The XPS results showed that increasing the temperature could also increase the Cr/Fe ratio in the passive film [Figure 4C][36]. However, the above conclusions were mostly drawn from electrochemical studies. Moreover, these structural changes require further verification.

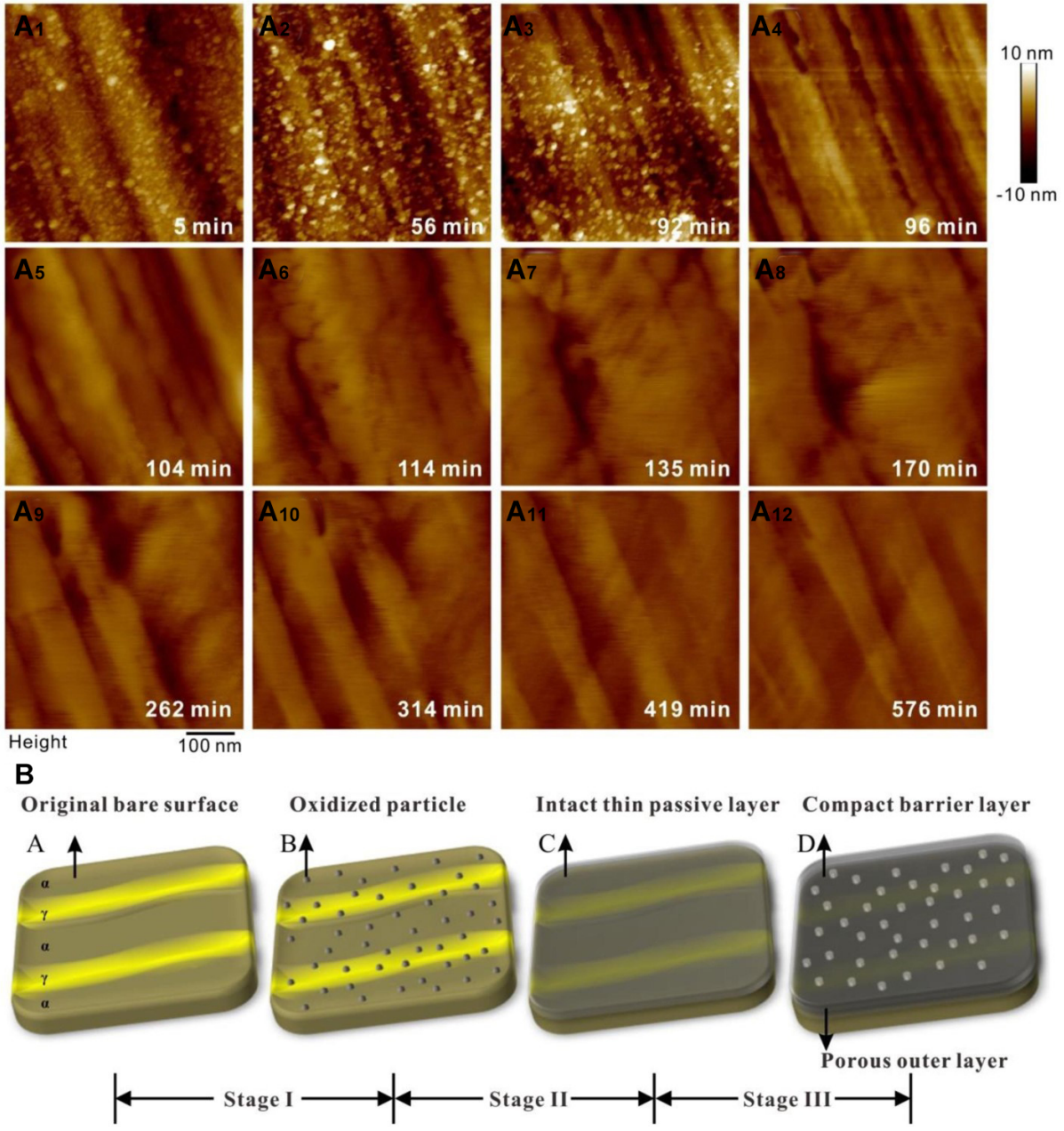

Figure 2. Evolution of the passive film on 2,205 duplex stainless steel[25]. (Open access). (A) The surface morphology changes within 600 min and (B) a schematic diagram of the passive film evolution.

Hydrostatic pressure is inevitable when considering the use of deep-sea counterparts. On the one hand, hydrostatic pressure decreases the Nyquist impedance and Cr_2O_3 proportion of the passive film [Figure 4D][37]. These changes indicate that hydrostatic pressure may reduce the compactness of the passive film[37]. On the other hand, potentiodynamic results show that hydrostatic pressure promotes the hydrogen evolution reaction by accelerating hydrogen adsorption on the metal surface and inhibiting the transfer of H_2 molecules[37]. However, the changes to the passive film due to hydrostatic pressure have not been adequately investigated. Therefore, elucidating the relationship between the changes in the passive film and the hydrogen evolution reaction may help clarify the mechanism. Cui *et al.* used the High Field Model and

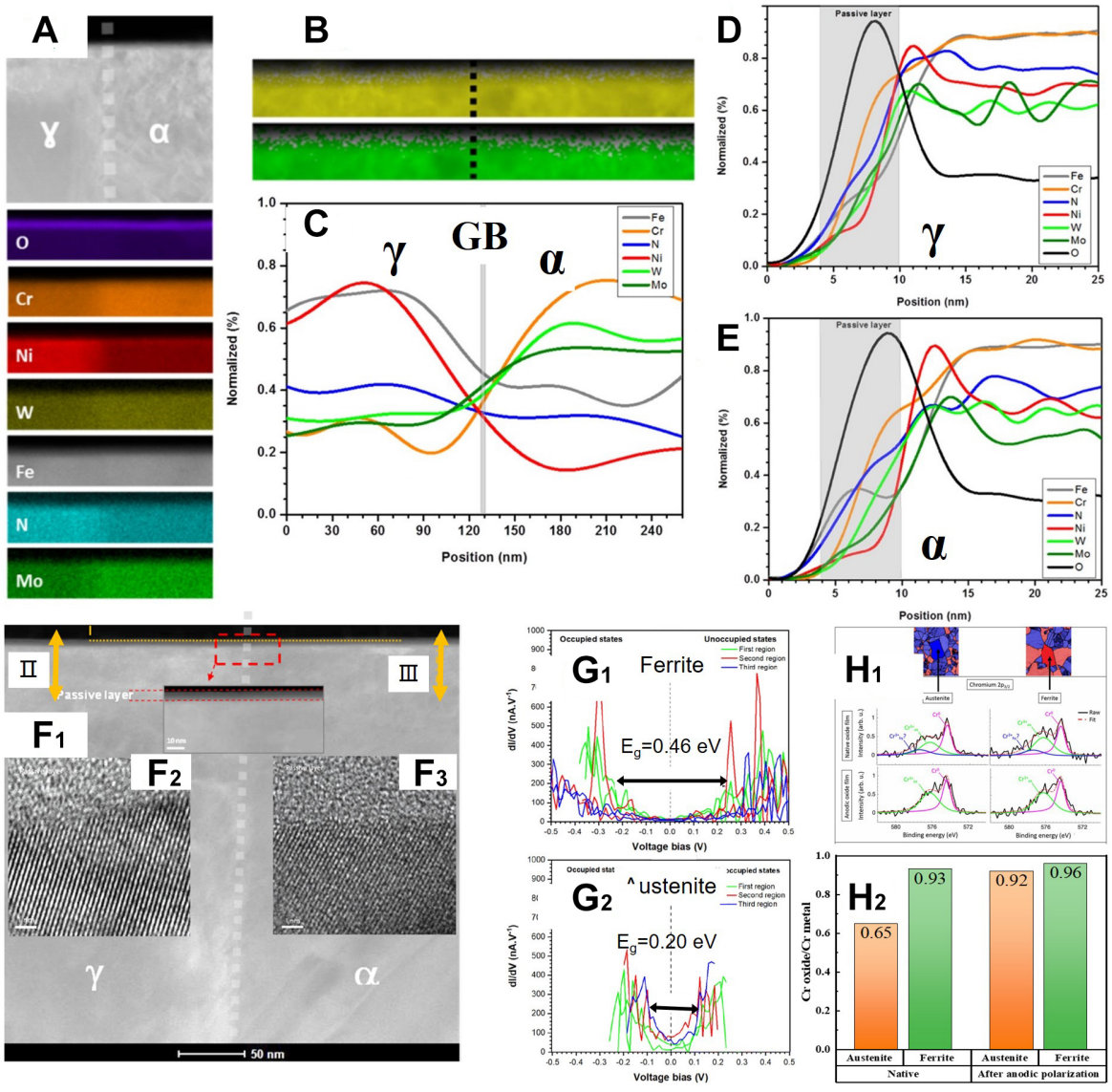

Figure 3. (A-C) EDS analyses revealed that the elements in the passive film are unevenly distributed. (Reproduced with permission[30]. Copyright 2019, Elsevier). Chromium, molybdenum and tungsten are enriched in the passive film on the ferrite phase. Nitrogen and nickel are enriched in the passive film on the austenite phase. (D and E) Line-scanning from the passive film to the matrix revealed that nickel is enriched at the film/matrix interface. (Reproduced with permission[30].Copyright 2019, Elsevier). (F) FIB analyses demonstrated that the passive film thicknesses of ferrite and austenite phases are already the same. (Reproduced with permission[30]. Copyright 2019, Elsevier). (G_1 and G_2) Scanning tunneling spectroscopy (STS) results show that the energy gap (E_g) of passive film on the ferrite phase is higher than that of the austenite phase, which means that passive film on the ferrite phase has a higher local energy gap between different semi-conductive characteristics (local conduction band potential and local valence band potential) (Reproduced with permission[30].Copyright 2019, Elsevier). (H_1 and H_2) The chromium oxide content of the passive film on the ferrite phase is higher than that on the austenite phase[29]. (Open access).

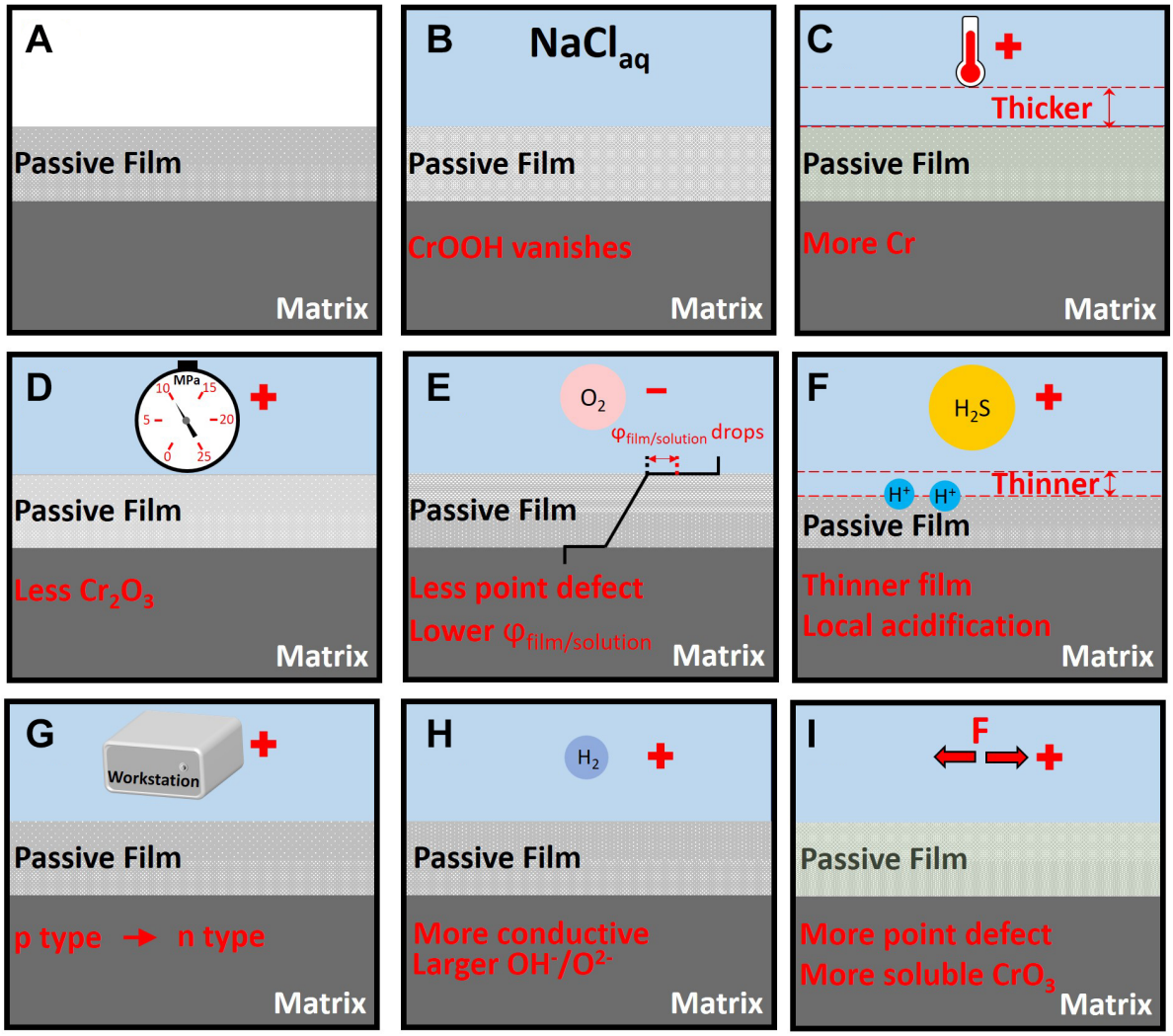

Figure 4. The effect of environmental variables on the passive film. (A) The passive film in the open air is constituted by a two-layer structure, specifically, the Cr-rich inner layer and the Fe-rich outer layer. (B) When immersion in the solutioncontaining chlorides, the CrOOH disappears[28]. (C) When the temperature increases, the passive film thickens and becomes more enriched in Cr[35]. (D) When the hydrostatic pressure increases, less Cr_2O_3 is detected[37]. (E) Removing oxygen decreases the point defects in the passive film and lowers the film/solution potential drop[35]. (F) Hydrogen sulfide accelerates the film dissolution process and local acidification processes[38]. (G) Increasing the anodic potential transforms the passive film from p-type to n-type[36]. (H) Hydrogen charging makes the passive film more conductive and imparts it with a larger OH^-/O^{2-} ratio[39,40]. (I) Stress creates more point defects and more soluble CrO_3 in the passive film[41,42].

Point Defect Model (PDM) and proposed that reducing the oxygen content in the solution can reduce the potential difference of the field/substrate interface and decreases the point defect diffusivity [Figure 4E][35].

Hydrogen sulfide generates hydrogen ions via the reacidification effect [Figure 4F][38]. Adding hydrogen sulfide does not change the semiconductor type of the passive film, but thins the film [Figure 4F][38]. A higher anodic current indicates that it accelerates the dissolution of the passive film. When the concentration was increased, the number of oxygen vacancies increased and Fe^{2+} in the passive film was consumed.

The influence of the applied potential on the passive film can be divided into anodic potentials and cathodic potentials, compared with the corrosion potential. One research strategy is focused on the composition change. At low anodic potentials, the passive film exhibits p-type semiconductor characteristics, because the passive film is composed of Cr_2O_3, FeO, NiO, and MoO_2, which contain many cationic vacancies. At high anodic potentials, the main components are Fe_2O_3, FeOOH, CrO_3, and MoO_3. The passive film resembles the n-type semiconductor [Figure 4G][36]. Therefore, the conductivity of the passive film decreases when the applied anodic potential increases[36]. Another research thought focuses on the film evolution modes under applied potentials[35]. At low anodic potentials, the passive film grows and thickens. When the applied potential shifts to the transpassive potential range, electron removal increases the number of the valent species and the passive film dissolves.

The applied cathodic potential is related to the hydrogen evolution reaction. Time-of-flight secondary ion mass spectrometry (TOF-SIMS) analyses showed that hydrogen accumulates preferentially on the grain boundaries and phase boundaries of the duplex stainless steel[39]. *In situ* AFM revealed that hydrogen charging causes a height difference on the sample surface[39]. Further studies showed that hydrogen-charged specimens exhibit an increased conductivity, and that the increase in conductivity in the austenite phase is larger than that in the ferrite phase[40]. The composition analysis of the passive film demonstrates that hydrogen charging promotes the presence of oxygen atoms in the form of hydroxide [Figure 4H][39,40].

Elastic stress and tensile stress both increase the donor and acceptor densities as determined using Mott-Schottky measurements [Figure 4I][41,42]. Stress increases the number of dislocations on the surface. According to the PDM models, dislocations promote the formation of vacancies in passive films[42].

In summary, the study on the environmental response of passive films focuses on their semiconductor properties, compositions, and structural response characteristics. As the thickness of the passive film is only a few nanometers, the above parameters are mostly obtained by substituting the macroscopic data into the existing model. Therefore, its accuracy is debatable. The specific evolution process of the influence of environmental factors on passive films is not clear. Further research can be conducted using high-resolution observation methods coupled with an environmental test bench.

Degradation of the passive film

It was believed that the rupture of the passive film was caused by the reaction from the trivalent chromium to the soluble tetravalent chromium at a certain potential, which was consistent with the sudden current increase. However, new experimental results do not support this view. Using *in situ* synchrotron grazing-incidence X-ray diffraction (GIXRD), a new phenomenon was observed that the passive film would thicken, accompanied by accelerating iron dissolution, and crystallinity decreases of the passive film when the potential increased in the passivation zone [Figure 5A-D][43]. This indicates that the rupture of the passive film is not only a valence change process but also a structural change process. As the applied potential increases to the breakdown potential, the composition and structure change simultaneously. Chromium, nickel and molybdenum in the passive film react and form soluble substances [Figure 5E and F][44]. The passive film becomes loose, whereas the film/matrix interface becomes dense owing to the enrichment of nickel and molybdenum[44]. These phenomena indicate that the rupture process of the passive film is a continuous degradation process over a wide potential range, rather than a sudden change as per the traditional definition [Figure 5G][44].

Nevertheless, there are also some factors that still need to be defined. Firstly, the difference in the degradation process of passive film between the austenite and ferrite phases is not fully understood. The

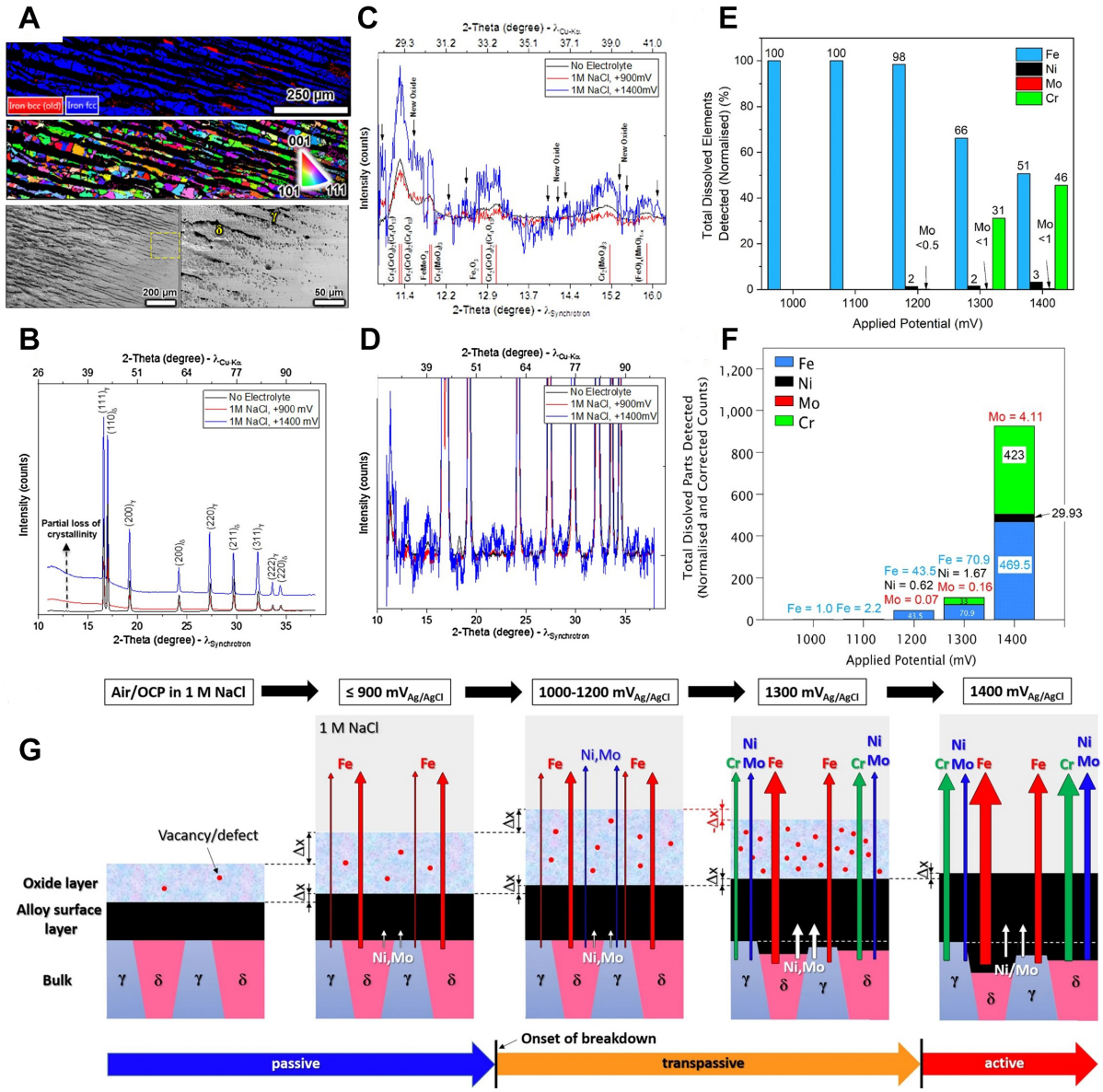

Figure 5. Study of the passive film degradation of duplex stainless steel after anodic polarization at 900 and 1400 mV (*vs.* Ag/AgCl) in 1 M NaCl (aq). (A) During the polarization test, selective dissolution occurred on the ferrite phase and the austenite phase was corroded as well. (Reproduced with permission[43].Copyright 2018, Elsevier). (B) The main composition was ferrite and austenite.(Reproduced with permission[43].Copyright 2018, Elsevier). (C) The small diffraction peaks corresponded to multiple crystal oxides (Reproduced with permission[43].Copyright 2018, Elsevier). (D) Chromium oxide is the major compound of crystal oxides. The random noise represents the nano-crystalline structure of the oxides. (Reproduced with permission[43].Copyright 2018, Elsevier). (E and F) The X-Ray Fluorescence (XRF) data for Fe, Cr, Ni, and Mo after applying different anodic polarization at room temperature[44].(Open access). (G) The degradation mechanism of 2,507 duplex stainless steel under the applied potential[44].(Open access).

studies mentioned above were conducted on the entire surface of the samples, and the exact phases cannot be distinguished. The morphological results show that both ferrite and austenite are corroded[43]. Secondly, the hydrogen evolution reaction, in addition to anodic polarization, could also degrade the passive film, since current research all focuses on the transpassive process of the passive film. This type of degradation is still not clearly understood. The mechanism by which the passive film changes if the hydrogen reaction occurs is yet to be explored.

PITTING CORROSION

The pitting corrosion mechanism includes both initiation and propagation mechanisms. The initiation and stabilization mechanisms of metastable pitting are still not comprehensively understood. Research on the pitting corrosion mechanism is mostly performed on single-phase austenitic materials, and there is little research on duplex stainless steel, which is more complicated. Current research on the pitting corrosion of duplex stainless steels mostly focuses on the correlation between various material factors with the pitting corrosion resistance and their mechanisms. These material factors include alloying composition and microstructure. As duplex stainless steels are mainly applied in chloride-containing environments, the default environment is a Cl-containing reducing environment unless specifically mentioned.

Alloying elements

Nitrogen element

Nitrogen is the element that solves the welding problems of duplex stainless steels and makes it widely commercially available. Nitrogen slightly increases the pitting potential and protection potential of duplex stainless steels[45]. When the nitrogen content in 2,507 is increased from 0.15 wt.% to 0.27 wt.%, the corrosion rate decreases by approximately 85%[46]. However, previous studies mainly focused on corrosion evaluation and not on the corrosion mechanism, and some topics remain debatable. Nitrogen is mainly distributed in the austenite phase in duplex stainless steels, and the solubility of nitrogen in the ferrite phase is extremely low. In austenitic stainless steel, nitrogen exists as NH_4^+ in the passive film[47]. Therefore, the addition of nitrogen leads to a larger difference between the Pitting Resistance Equivalence Number (PREN) values of the two phases. According to the point of view that the phase with the lowest PREN represents the pitting corrosion resistance, the addition of nitrogen has little effect on the pitting corrosion resistance, which is not consistent with the experimental results.

Molybdenum element

Molybdenum can significantly increase the pitting corrosion resistance of duplex stainless steels. When molybdenum content is below 1.0 wt.%, molybdenum exhibits no obvious improvement in pitting corrosion resistance[48]. However, adding 1.5 wt.% Mo can increase the pitting potential by at least 150 mV[49]. This is mainly attributed to two reasons. Firstly, molybdenum exists in the passive film in the form of MoO_2, MoO_3, and MoO_4^{2-}. These oxides render the passive film more stable[49]. Secondly, molybdenum accumulates in the pits and hinders further dissolution[50]. Additionally, Tian *et al.* found that tetravalent Mo species only exist in the passive film of 2,205 duplex stainless steel, as compared to single ferrite phase or single austenite phase[51]. This indicates that molybdenum plays an important role in the interaction between the austenite and ferrite phases. However, the exact interaction between the austenite and ferrite phases is unclear. The influence mechanism of molybdenum on austenite and ferrite in different stages of pitting corrosion still needs to be comprehensively understood.

Nickel element

Nickel changes the composition of the passive film by introducing metallic Ni, NiO, $Ni(OH)_2$, and $NiCl_2$[52]. This is beneficial for pitting corrosion resistance[46]. A nickel content of 5-13 wt.% increases the pitting potential in 1 M hydrochloric acid by 500 mV[53]. Nickel also narrows the protection potential range[53]. However, the content change of nickel causes a significant change in the ratio of the two phases[54], and the ratio of the two phases has a greater impact on the pitting corrosion ability. When studying the influence of nickel, it is necessary to control the ratio of the two phases by heat treatment. Additionally, the influence of nickel on pitting corrosion is still mainly observed using electrochemical tests, and comprehensive research needs to be conducted from the perspective of the corrosion morphology and the corrosion rate.

Tungsten element

Kim *et al.* reported that adding 4 wt.% tungsten increases the pitting potential and critical pitting temperature of the duplex stainless steel. It could also promote the repassivation process[52]. Tungsten exists as WO_3 and W^M in passive films. However, Torres *et al.* reported that adding 2.1 wt.% tungsten to the duplex stainless steel decreases the critical pitting temperature when aged at 920 °C for 60 s[55]. This change correlates with the fact that tungsten favors the precipitation of the chi phase. The opposite results that were obtained for tungsten are not only because the heat treatment varied but also because the steel used in the research was not a single variable. That is, industrial steels were used as the test samples[52,55], in which the contents of molybdenum, silicon and other elements vary, which also influences the pitting corrosion resistance and may obscure the influence of tungsten. Another study that controlled element tungsten more accurately showed that tungsten is slightly beneficial in resisting pitting corrosion when in the solid solution state[56]. However, tungsten is detrimental when detrimental phases containing tungsten precipitate.

Copper element

Copper exists in duplex stainless steels in the form of the solid solution state or epsilon-Cu, the latter of which exists when the sample is aged at 700-800 °C[57,58]. The addition of copper in the solid solution state has few beneficial or even negative effects[59]. Although copper is more stable than iron, the corrosion product of copper dissolves into complex ions containing Cu[57], which have not been fully understood until now. Epsilon-Cu has been reported to be more active than the ferrite and austenite phases[60], which means that it dissolves preferentially and forms nucleation sites for pitting corrosion. However, the electrochemical test is the main test method on this topic which cannot reflect the corrosion mechanisms microscopically. Additionally, *in situ* observation of the pitting corrosion process caused by epsilon-Cu is still lacking. The change in the pitting nucleation and pitting propagation stages after the addition of solid-solution copper is also vague.

Manganese element

Manganese exists in passive films in the form of oxidation states II and IIII[61]. Jang reported that adding 0.8 wt.% manganese to CD4MCU cast duplex stainless steel negatively impacts the pitting corrosion resistance, but the pitting corrosion resistance recovers by adding 2 wt.% manganese[62]. Jang attributed these changes to the proportion of austenite/ferrite[62]. Mass loss tests showed that increasing the manganese content from 1.7 to 3.3 wt.% significantly decreases the pitting corrosion resistance[49]. However, the pitting potential slightly increased when adding 8.03 wt.% in the solid solution state to duplex stainless steel[63]. Feng *et al.* reported that manganese is detrimental when aging at 800 °C for forming precipitants[64]. Therefore, it can be concluded that manganese increases the number of pit nucleation sites when it exists in the form of precipitants (inclusions or secondary phases). However, the current research shows that manganese-containing inclusions exhibit different dissolution modes, and the specific mechanisms of these different dissolution modes still need clarification. Additionally, existing studies have shown that solid-solution-state manganese does not seem to have a significant effect on the pitting corrosion of duplex stainless steels.

Titanium, niobium and tantalum

Titanium is a strong nitride-forming element which means TiN would form upon Ti is added to duplex stainless steels. Firstly, titanium could form TiN. Secondly, titanium in the solid solution state forms oxides. Zhang *et al.* has reported adding 0.01 wt.% titanium increased the pitting potential[65]. However, when 0.15 wt.% titanium was added, the pitting potential decreased. The authors attributed this change to the size of TiN. However, no direct evidence was provided to support this.

Adding 0.25 wt.% Nb to the duplex stainless steel increases the pitting potential by more than 100 mV. Niobium forms the Z phase that surrounds the anodic inclusions[66]. Furthermore, the Z phase has a low mismatch with the matrix, and there is no gap between the matrix and Z phases[66]. Therefore, niobium addition decreases the number of pitting nucleation sites.

It has been reported that tantalum additions can hinder the precipitation of harmful phases, which improves the pitting corrosion resistance[67,68]. Further studies showed that tantalum forms nitrides that coat the CaS and (Al, Ca) oxides. When CaS and (Al, Ca) oxides dissolve, stable nitrides containing tantalum prevents further propagation of pitting corrosion[69].

Other elements

Aluminum was found to have a negative effect on pitting corrosion. The negative effect is not obvious when contents are below 1 wt.%, but it is obvious when the contents are above 1.5 wt.%[70]. This is because the Al_2O_3 film formed by aluminum is porous. Studies have reported that Al_2O_3 forms an Al_2O_3 layer on the surface only when the content is above 4-6 wt.%.

The addition of 0.2 wt.% silver is detrimental to pitting corrosion resistance. Silver increases the fraction of secondary austenite[71]. Pits preferentially initiate at secondary austenite. Additionally, the solubility of silver in steel is very low, and pitting corrosion is preferentially initiated at the interface between the Ag-containing precipitates and the matrix.

Sulfur addition of 0.001 to 0.053 wt.% increases the pitting nucleation sites by approximately 3.5 times[72]. Manganese sulfides increase significantly, which deteriorates the pitting corrosion resistance. The pitting potential decreases by approximately 700 mV in 3 M NaCl[72].

Rare earth metals (REMs) exist in duplex stainless steels in the form of precipitates. The addition of REMs can refine polygonal Mn inclusions into uniform-shaped REM oxides[73]. These REMs oxides are ball-shaped at the interface and act as cathodes during corrosion[74]. Pitting corrosion occurs at the matrix near the oxide/matrix interface, rather than at the oxide[74]. The frequency of metastable pitting also decreases[74]. However, Kim *et al.* did not clarify why pitting corrosion initiates in the matrix near the oxide/matrix interface instead of in the matrix away from the REM oxides[74].

Adding 0.01-0.2 wt.% tin was also found to improve corrosion resistance, and its effect was better when it was compounded with copper[75], but the specific mechanism is still unclear.

Ruthenium addition of approximately 0.28 wt.% can increase the pitting corrosion potential in sulfuric acid by 100 mV[76]. The passive current decreases dramatically with the addition of ruthenium. This indicates that ruthenium can hinder anodic dissolution. However, in the only report on this topic, the conclusion was mainly drawn using macroscopic electrochemistry and weight loss, and the partition and influence mechanism of ruthenium between the two phases is yet to be understood.

In summary, the mechanism of alloying elements on the pitting corrosion of duplex stainless steels can be roughly divided into six mechanisms. In the stabilization mechanism [Figure 6A][49], elements accumulate in the passive film and at the bottom of pits, which stabilize the passive film and hinder further dissolution in the corrosion pits. This mechanism has been verified for molybdenum in the solid solution state[49]. In the ineffective mechanism [Figure 6B][49,59], the element does not stabilize or deteriorate the passive film. When pitting corrosion propagates, this kind of element is also corroded. This mechanism applies to manganese

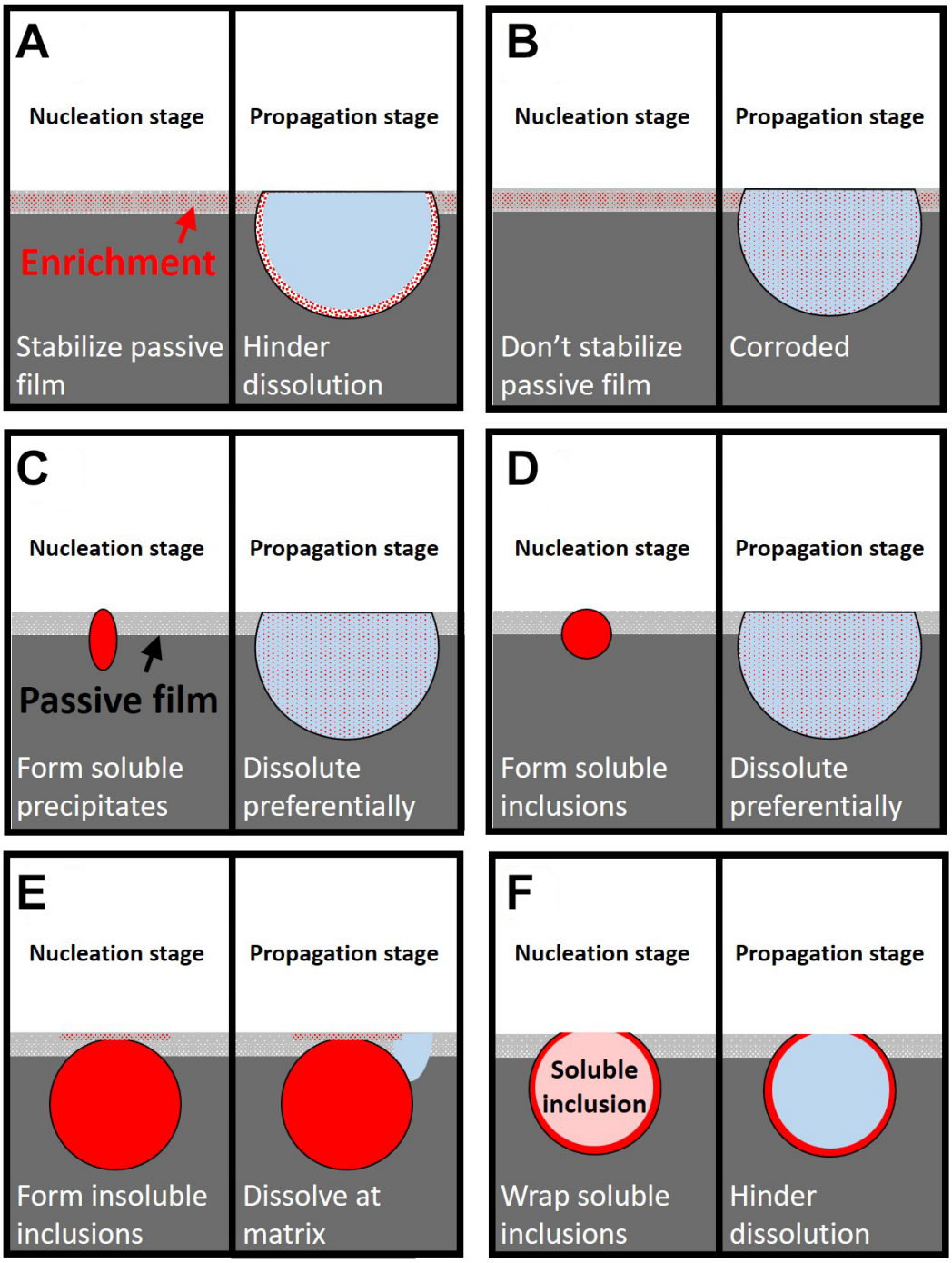

Figure 6. The six mechanisms of alloying elements on the pitting corrosion of duplex stainless steels. (A) Stabilize the passive film and hinders further dissolution in the corrosion pits. This mechanism has been verified for molybdenum[49]. (B) Does not stabilize or deteriorate the passive film. When pitting propagates, the element is also corroded. This mechanism applies to both manganese[49] and copper[59] in the solid solution state. (C) Forms soluble precipitates, which dissolve preferentially and nucleate pits. This mechanism applies to copper after aging during which epsilon-Cuis formed[60]. (D) Forms soluble inclusions. The inclusions dissolve preferentially and nucleate pits. This mechanism is applied to sulfur[72]. (E) Forms insoluble inclusions, which do not corrode. Pitting corrosion occurs in the matrix near the inclusions. This mechanism has been reported for titanium[65]. (F) Wraps soluble inclusions. When the inclusions dissolve, the protective layer protects the matrix from pitting corrosion. This mechanism applies to adding niobium[66].

and copper in the solid solution state[57]. In the soluble precipitates mechanism [Figure 6C][60], the element preferentially promotes the formation of soluble precipitates and dissolves, promoting pit nucleation. This mechanism applies to copper after aging during which epsilon-Cu is formed. Epsilon-Cu corrodes and initiates pitting[60]. In the soluble inclusions mechanism [Figure 6D][72], the alloying elements forms soluble inclusions. The inclusions preferentially dissolve and nucleate pits. This mechanism applies to the addition of sulfur[72]. In the insoluble inclusions mechanism [Figure 6E][65], the alloying elements form insoluble inclusions, which do not corrode. Pitting corrosion occurs in the matrix near the inclusions. This mechanism has been previously reported for titanium[65]. The last mechanism is the wrapping mechanism [Figure 6F][66]. The element forms a protective layer that wraps the soluble inclusions. When the inclusions dissolve, the protective layer protects the matrix from pitting corrosion[66,69].

Microstructure

Ferrite and austenite

The Volta potential difference between the ferrite and austenite phases is approximately 50-100 mV [Figure 7A][28,77]. The potentiodynamic results show that the dissolution potentials of austenite and ferrite are -281 mV_{SCE} and -323 mV_{SCE} in 1 M H_2SO_4, respectively[78]. Theoretically, the potential difference should induce micro-galvanic corrosion and accelerate the corrosion of the ferrite[79]. However, duplex stainless steel has excellent corrosion resistance. Xiao proposed that there is feedback during the corrosion process[80]. The corrosion of the ferrite phase can change the passive film of the austenite phase. Xiao also believed that the potential difference is no longer the main electrochemical inhomogeneity in corrosive media, where both phases can be passivated[80]. Tian *et al.* found that the passive current density of the duplex stainless steel was lower than that of the single-phase structure[51]. The two phases in the duplex stainless steel may interact during the corrosion process. Cheng *et al.* found that the defect density in the two-phase passive film is lower than that of single austenite phase or single ferrite phase[81]. They proposed that the two-phase galvanic corrosion effect improves the corrosion resistance of the duplex stainless steel. However, the exact galvanic corrosion mechanism is unclear. Additionally, the existing test methods are controversial. The single-phase structure obtained by anodic dissolution is honeycomb-like. Therefore, the single-phase samples have more interfaces, which increases the risk of crevice corrosion of the samples during electrochemical testing.

Pitting corrosion after deformation has also been studied[28,78]. Örnek and Engelberg reported that the ferrite phase of 2,205 undergoes pitting corrosion preferentially before cold deformation, whereas the austenite phase preferentially pits after a 40% cold deformation[77]. Luo *et al.* also found that when the cold deformation of UNS S31803 exceeds 70%, pitting corrosion preferentially initiates in the austenite phase[82]. Molyndal *et al.* proposed that the corrosion resistance of ferrite decreases monotonically with strain but not in the austenite phase[78]. Slip bands and subgrains are formed in austenite under a small deformation, which barely deteriorate the pitting corrosion resistance. High-angle grain boundaries are formed in austenite under large deformation, which deteriorates the pitting corrosion resistance[78]. Therefore, the relative pitting corrosion resistance between ferrite and austenite reverses as the cold deformation increases [Figure 7B1 and B2][83]. However, the above studies were based on the correspondence between pitting corrosion behavior and microstructural changes after deformation. Evidence for the direct correlation between microstructural changes (dislocation configuration, slip banding, and subgrain boundaries) and pitting corrosion is still lacking.

The phase ratio affects the pitting corrosion as well [Figure 7C1 and C2][23]. Ha *et al.* stated that the smaller the PREN difference between the two phases, the stronger the pitting corrosion resistance of the entire matrix[21,22]. This view was verified in 2,205 and 2,101 duplex stainless steels. However, the pitting corrosion resistance of different phase ratios in 2,507 stainless steel The pitting corrosion resistance with different

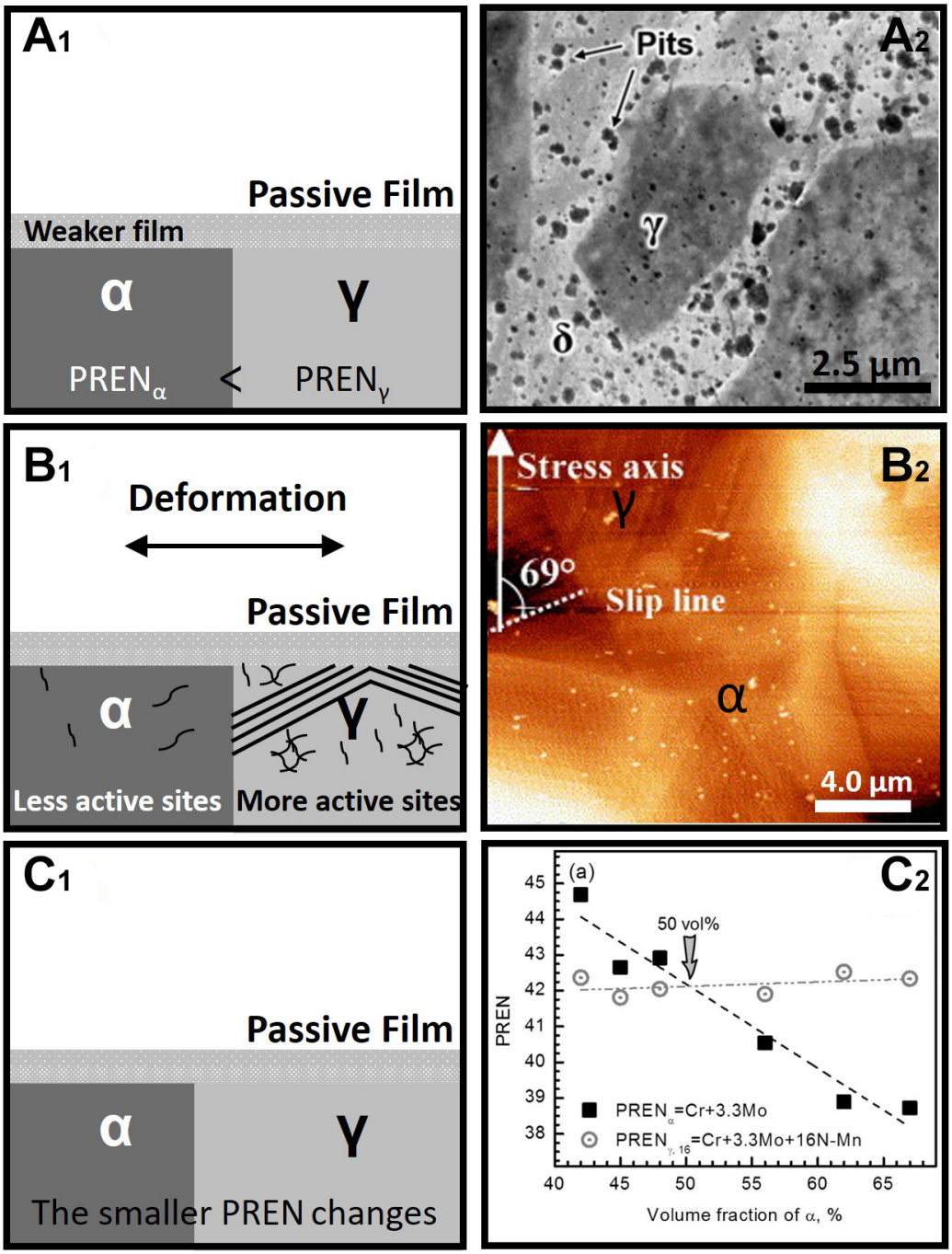

Figure 7. Summary of the studies on the pitting corrosion resistance between ferrite and austenite. (A_1) The pitting resistance equivalent number of the ferrite phase is smaller than that of austenite. Therefore, the passive film of ferrite is unstable, and pitting corrosion occurs preferentially in ferrite. (A_2) In the chloride-containing environment, the amount of pitting corrosion initiated in the ferrite phase is significantly more than that in the austenite phase[28] (Open Access) (B_1) Under plastic deformation conditions, austenite forms more dislocation walls, slip bands, and dislocation outcropping defects. Therefore, more active sites appear on the surface of the austenite phase, and the pitting corrosion resistance gap between ferrite and austenite becomes smaller and even reversed. (B_2) After plastic deformation, the defects in austenite increase significantly, whereas that in the ferrite phase changes little. (Reproduced with permission[83]. Copyright 2006, Elsevier). (C_1) Element diffusion occurs during the heat treatment process to change the phase ratio. The minimum value of the pitting resistance equivalent number changes, and the pitting corrosion resistance of duplex stainless steel changes. (C_2) UNS S32750 with different phase ratios exhibits different pitting potentials. (Reproduced with permission[23]. Copyright 2015, Elsevier.

phase ratios is not highly correlated with PREN. but it is well correlated to the two-phase micro-galvanic corrosion depth[23]. The authors believed that this is because PREN mainly reflects the initiation process of pitting corrosion. This is suitable for 2,205 and 2,101 duplex stainless steels, which are not resistant to pitting corrosion. The corrosion resistance of 2,507 duplex stainless steel is higher. Therefore, the pitting corrosion performance mainly depends on the pitting propagation process. However, according to the pitting corrosion model proposed by Li *et al.* and Frankel *et al.*, the propagation process plays a decisive role in materials that are not resistant to corrosion[84,85]. This opinion contradicts that of Ha *et al.*[21,22]. However, the model proposed by Li *et al.* has not been verified in the duplex stainless steel system[84,85]. Therefore, the mechanism of the phase ratios on the pitting corrosion requires further clarification.

Precipitates

Harmful phases precipitate in duplex stainless steels during welding and isothermal aging processes. In metals, precipitates typically have a deleterious effect on pitting resistance[86]. There are three opinions on interpretations of the pitting corrosion mechanisms of secondary precipitates.

The first theory is the Cr-depletion theory [Figure 8A1], where the precipitates are enriched with chromium or molybdenum, which forms a surrounding depleted zone. The passive film at the depleted zone is weak or absent. Pitting corrosion occurs in these areas. This theory is applicable to secondary austenite, sigma phase (σ phase), chi phase (χ phase), CrN, and Cr_2N [Figure 8A2 and A3][87-90]. Zhang *et al.* showed that after tempering at 700 °C for a sufficient duration, the pitting initiation site of S82441 duplex stainless steel transformed from austenite to the Cr-depleted zone[91]. The higher the quantity of the sigma phase, the lower the breakdown potential. However, the pitting corrosion resistance recovers to a certain degree after aging for a sufficient time. Once the sigma phase is fully precipitated, further aging causes tungsten and molybdenum to diffuse into the Cr-depleted secondary austenite[92].

The Cr-depleted α phase formed by spinodal decomposition can also induce pitting corrosion, but it is not as strong as the σ phase[93]. The micro-galvanic corrosion model has been proposed to interpret this phenomenon [Figure 8B1][94,95]. Cathodic phases enriched in chromium surround anodic phases depleted in chromium [Figure 8B2 and B3][94]. Microgalvanic corrosion induces pitting corrosion in the Cr-depleted phase, which has been proposed recently and is appliable to the α and α' phases.

The pitting corrosion that occurs around the G phase is still under debate. The stress concentration model assumes that a large strain field is generated around the square precipitate, which promotes the initiation of pitting corrosion preferentially at this location [Figure 8C1]. A high-stress field has been verified using HAFFT [Figure 8C2 and C3][96]. Another hypothesis is that pitting corrosion is related to the Cr-depleted zone around the G phase, which is caused by the growth of the G phase. Silva *et al.* recently suggested that the pitting corrosion around the G phase is due to galvanic corrosion[94].

In summary, research on microscale precipitates and nanoscale precipitates has yielded a unified understanding of the σ and χ phases, whereas the knowledge of nanoscale precipitates, such as the G phase, α phase and α' phase, is still lacking. Transmission electron microscopy (TEM) has been adapted to trace the initiation sites and propagation tendency in austenite stainless steel and got good results on Cu-rich phases and MnS[97]. This technology is promising in studying the pitting corrosion related to nanoscale precipitates in duplex stainless steel. The second tendency is from static research to dynamic research. The precipitation growth process of secondary phases leads to the diffusion of alloying elements, which affects the pitting corrosion resistance. Moreover, research on the surface passive films of the precipitates is still lacking. Current research has reported that TiB_2 nanoparticles help suppress pitting initiation, because it is easier to

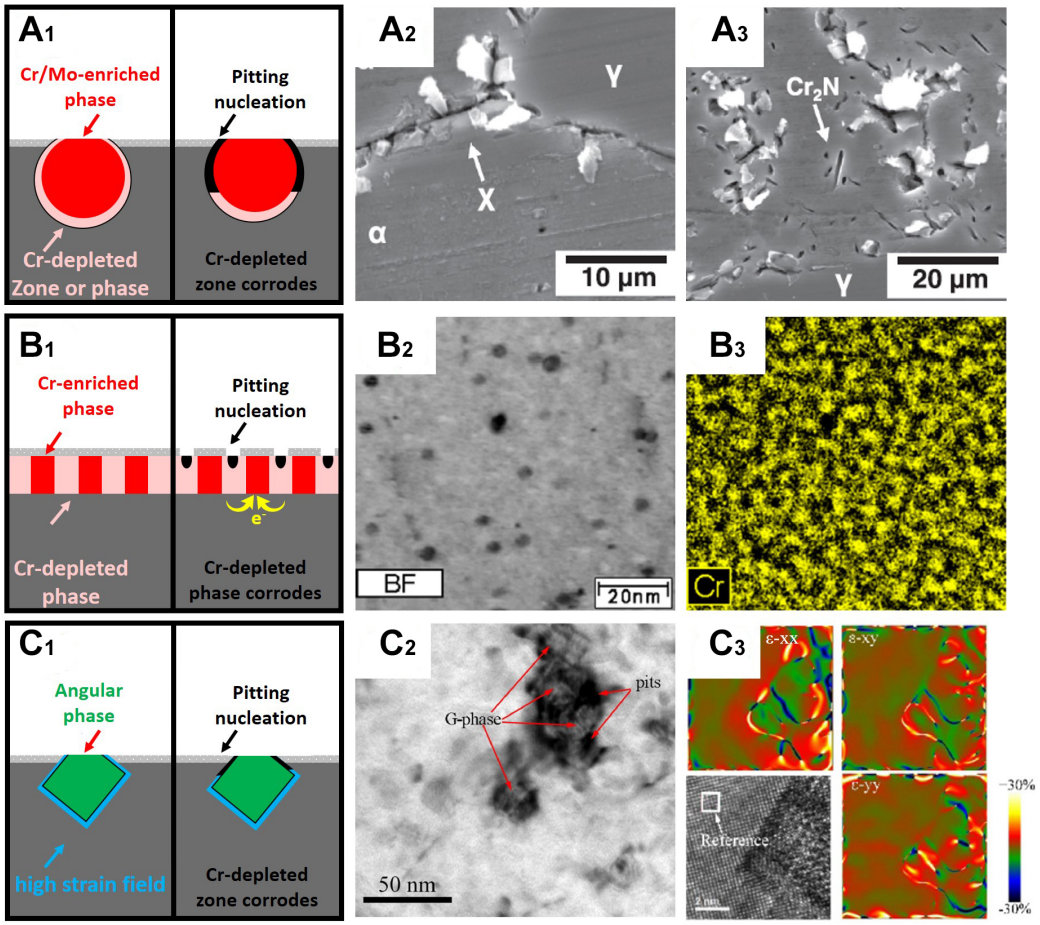

Figure 8. The proposed pitting corrosion mechanisms of the precipitants. (A) When secondary phases are enriched in chromium or molybdenum, a surrounding depleted zone is formed. The passive film at the depleted zone is weak or absent. Pitting corrosion occurred at the Cr-depleted zone. This theory is applicable to σ phase, χ phase and CrN. (Reproduced with permission[87]. Copyright 2014, Elsevier). (B) Cathodic Cr-enriched secondary phases surround anodic Cr-depleted phases. The micro-galvanic corrosion induces pitting corrosion in the Cr-depleted phase. This theory has been recently proposed and is applicable to α and α′ phases. (Reproduced with permission[94]. Copyright 2022, Elsevier). (C) A large strain field is generated around the square precipitate, which promotes the initiation of pitting corrosion preferentially at this location. (Reproduced with permission[96]. Copyright 2020, Elsevier). This opinion has been proposed to interpret the pitting corrosion around the G phase, which is still under discussion.

passivate[98]. This research indicates that the passive film on the precipitates is meaningful for further understanding the role of precipitates in pitting corrosion.

ENVIRONMENTALLY-ASSISTED CRACKING

The main causes of EAC in duplex stainless steels are chloride-induced stress corrosion cracking, hydrogen-induced stress cracking, and sulfide stress cracking, which was deduced from the failure investigation in the Introduction Section. These failures are caused by a combination of the anodic dissolution mechanism and the hydrogen embrittlement mechanism. Additionally, the stacking fault energy of the austenite phase is significantly lower than the ferrite phase. Dislocations cross-slip more easily in austenite. Therefore, dislocations move differently between the phases. This causes the crack to propagate in different ways between the phases. Nevertheless, there is a lack of discussion on this important topic.

Environmentally assisted cracking (EAC) is the main failure cause in duplex stainless steel. EAC is caused by the combined effects of materials, stress, and a corrosive environment[99]. At the mesoscopic scale, the suggested mechanisms include: (1) The anodic dissolution mechanism, which suggests that the nucleation and propagation of cracks result from the preferential dissolution of atoms at the crack tip[100]; (2) The adsorption-induced dislocation emission theory, where absorbed ions reduce the bonding force of the atoms at the crack tip, which promotes dislocations nucleation. Dislocations connect the holes, thereby inducing crack propagation[101]; (3) The weak bond theory, where hydrogen atoms generated by the electrochemical reaction are adsorbed at the crack tip. Hydrogen reduces the bonding force between the atoms at the crack tip and promotes crack propagation[102]; (4) Hydrogen promotes local plastic deformation theory. Hydrogen promotes the movement of dislocations in the plastic zone. Therefore, slip/microvoids accumulate in the local plastic deformation zone and the crack propagates[103]; and (5) The membrane rupture theory, which assumes that the crack tip moves because the brittle product film at the crack tip ruptures under the action of an external force[104].

This section reviews the mechanisms and the recent studies on the main type of failures [Figure 9][105-109]. Overall, research on the EAC mechanism in duplex stainless steels is still lacking. The current research mainly focuses on how environmental variables affect EAC susceptibility.

Chloride-induced stress corrosion cracking

Although duplex stainless steel is more resistant to stress corrosion cracking than austenitic stainless steel, it still suffers from chloride-induced stress corrosion cracking under certain conditions[4], which include seawater and alkaline environments[110]. The cracking mechanism of chloride-induced stress corrosion cracking is associated with ferrite dissolution and hydrogen embrittlement[105]. The mechanism states that in the chloride-containing environments, chloride ions penetrate the passive film of duplex stainless steel [Figure 9A1 and A2]. Owing to the poor stability of the passive film, pitting corrosion is preferentially initiated in the ferrite phase. An autocatalytic effect occurs at the bottom of the pits, which hinders the repassivation of the matrix [Figure 9A3][105]. Under the action of stress, cracks initiate at the bottom of the pits. Distinct chloride-induced cracks are branched. When cracks propagate into the austenite phase, they are arrested [Figure 9A4][105]. Therefore, the cracks mainly propagate along the ferrite/ferrite boundaries and austenite/ferrite phase boundaries.

Wu *et al.* reported that the sensitivity of 2,205 duplex stainless steel in a simulated marine atmosphere increases with a decrease in the pH, and the main control mechanisms are the anodic dissolution mechanism and the hydrogen embrittlement mechanism[111]. The susceptibility of 2,101 duplex stainless steel increases with increasing temperature, then decreases when the temperature is above 50 °C[106]. This is because high temperatures intensify the anodic dissolution and weaken the hydrogen embrittlement[106]. The addition of 5,600 ppm of nitrate prolongs the rupture time of 2,507 duplex stainless steel in 30 wt.% $MgCl_2$ by nine-fold because it can reduce the adsorption sites of chloride ions[112].

The crack propagation resistance of ferrite is weaker than that of austenite[113]. However, some researchers believe that the anodic dissolution crack initiation in ferrite is not due to pitting corrosion. Wickström suggested that the chloride-induced cracks in ferrite in water droplet evaporation experiments were due to surface dealloying[114]. Not all circumstances make the ferrite more prone to chloride-induced stress corrosion cracking. For example, Örnek found that the austenite in 2,205 duplex stainless steel suffers from chloride-induced stress corrosion cracking in the drop test[115].

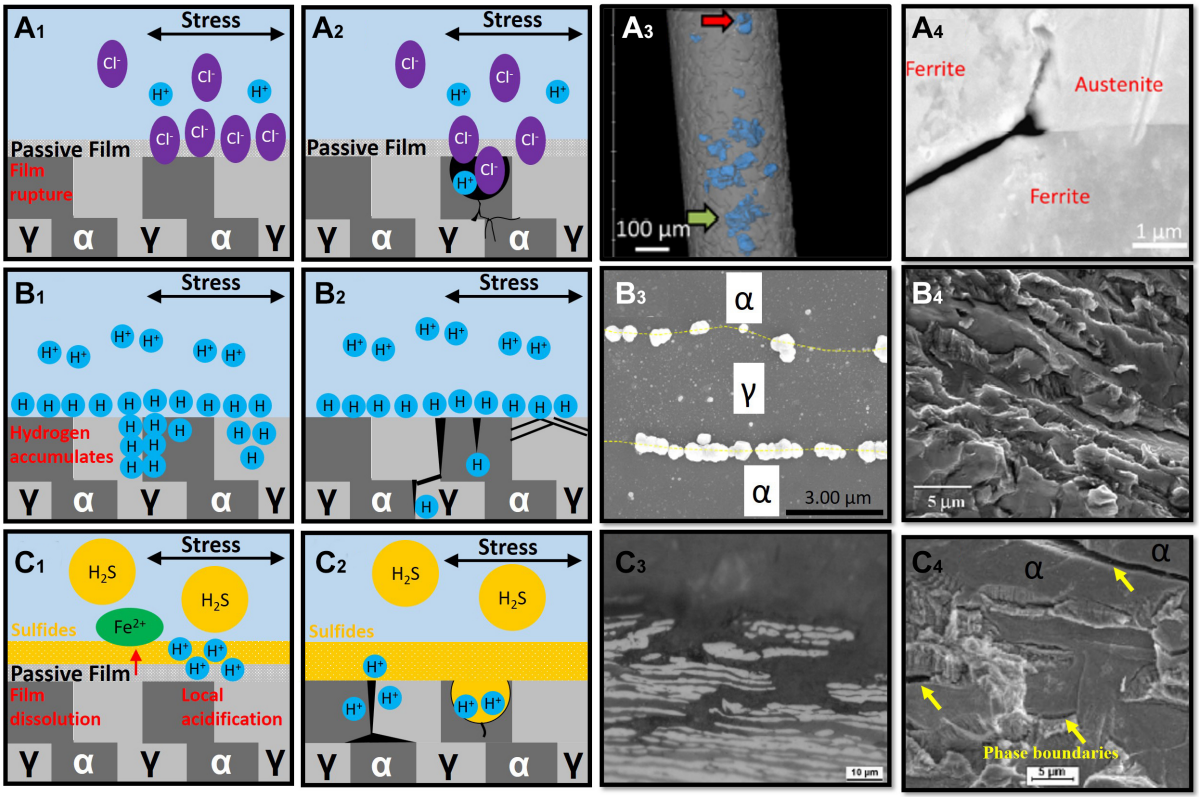

Figure 9. The mechanisms of (A_1-A_4) chloride-induced stress cracking, (B_1-B_4) hydrogen-induced stress cracking (C_1-C_4) and sulfide stress cracking. (A_1) In chloride-containing environments, chloride ions penetrate the passive film of the duplex stainless steel. (A_2) Due to the poor stability of the passivation film, pitting corrosion is preferentially initiates in the ferrite phase, and the autocatalytic effect occurs at the bottom of the pits, which hinders the repassivation of the matrix and initiates cracks under the action of stress. The crack is branched and stops when it propagates into the austenite phase. The crack propagates along the ferrite and austenite/ferrite phase boundaries. (A_3) Three-dimensional pitting corrosion on the surface of the duplex stainless steel. (Reproduced with permission[105]. Copyright 2021, Elsevier). (A_4) The crack blunts when it reaches the austenite phase and propagates along the ferrite and phase boundaries. (Reproduced with permission[105]. Copyright 2021, Elsevier). (B_1) Hydrogen atoms diffuse and accumulate at the phase boundaries. (B_2) Cracks initiate in the ferrite phase and ferrite/austenite phase boundaries and propagate in a zig-zag manner. Hydrogen promotes dislocation slip in austenite. (B_3) Hydrogen accumulates at the ferrite/austenite boundaries (Reproduced with permission[107]. Copyright 2022, Elsevier). (B_4) Both cracked ferrite and austenite exhibit brittle fracture characteristics. (Reproduced with permission[108]. Copyright 2006, Elsevier). (C_1) In sulfide environments, the passivation film dissolves and a layer of sulfide is formed on the surface. The surface is partially acidified, and the acidification effect produces corrosion. (C_2) Corrosion pits are formed in the ferrite phase. The reacidification and the autocatalytic effects generate hydrogen. Cracks initiate in the ferrite phase. Hydrogen generated at the corrosion product/substrate interface also preferentially diffuses to the phase boundaries and initiates cracks. (C_3) A sulfide corrosion product film forms on the surface of the sample, and the ferrite phase preferentially dissolves. (Reproduced with permission[106]. Copyright 2014, Elsevier). (C_4) Secondary cracks preferentially initiate at the phase boundaries and ferrite (Reproduced with permission[109]. Copyright 2006, Elsevier).

Hydrogen-induced stress cracking

Hydrogen-induced stress cracking mainly occurs under the conditions of the low cathodic protection potential and the deep-sea environment[116]. The mechanism is as follows. Hydrogen atoms diffuse and accumulate at the phase boundaries [Figure 9B1 and B3][107]. The decohesion effect of hydrogen causes the boundaries and planes to crack more easily [Figure 9B2]. A combination of the applied stress and the residual stress cause the specimen to crack. The cracks initiate in the ferrite phase and at the ferrite/austenite phase boundaries [Figure 9B4][108,117],which then propagate in a zig-zag manner[108].

Hydrogen charging in the pre-strained duplex stainless steel can induce dislocation multiplication[118]. Hydrogen can cause more obvious lattice deformation in austenite than ferrite[119]. Further studies interpreted this phenomenon by stating that hydrogen causes slip planarity and martensite formation in austenite[120,121]. Larsson *et al.* reported that hydrogen absorption causes compressive strains without stress[122]. This may be due to the expansion effect after austenite accommodates more hydrogen atoms.

The solubility of hydrogen atoms in the ferrite phase is significantly lower than that in austenite, whereas the diffusion rate in ferrite is considerably faster than that in austenite. Therefore, the ferrite phase is more prone to cracking during hydrogen embrittlement[123]. The remarkable role of the phase boundaries in hydrogen-induced stress cracking was recently recognized. The binding energies of phase boundaries, ferrite boundaries and austenite boundaries are 43.6, 26.5, and 13.5 kJ/mol, respectively[107]. Wu *et al.* used experiments, numerical simulations, and theoretical analysis to demonstrate that the phase boundaries are not only strong hydrogen traps but also act as fast hydrogen diffusion pathways[107].

Sulfide stress cracking

Sulfide stress cracking is common in the petrochemical industry. The occurrence of sulfide stress cracking is related to the dissolution of the passive film, sulfide formation, localized corrosion, and hydrogen embrittlement[124]. In the sulfide environment, the passivation film dissolves, and a layer of sulfide is formed on the surface[124]. The surface is partially acidified, and the acidification effect results in corrosion [Figure 9C1 and 9C3][106]. Corrosion pits are then formed in the ferrite phase. The reacidification and the autocatalytic effects generate hydrogen atoms. Cracks initiate in the ferrite phase [Figure 9C2]. Hydrogen atoms generate at the corrosion product/substrate interface also preferentially diffuse to the phase boundaries and initiate cracks [Figure 9C4][109].

Zucchi reported that adding sulfide to seawater increases the cracking sensitivity of 2,205 duplex stainless steel in neutral seawater[108]. The main control mechanism is the hydrogen embrittlement mechanism. The sensitivity of 2,101 duplex stainless steel after adding 10^{-3} M thiosulfate to a 20 wt.% NaCl environment is as high as 40%, but when the pH is increased to above 4.5, 2,101 is not sensitive to 10^{-2} M thiosulfate[106]. This indicates that the sulfide stress cracking is closely related to the acidification effect. The σ phase, which preferentially precipitates in the ferrite phase, also easily becomes the initiation point. The σ phase may crack first and the crack spreads along the interface between the ferrite phase and the σ phase[125].

CONCLUSIONS

This article first summarizes the failures in the last 20 years and identifies the main corrosion-related types leading to failures of duplex stainless steels. Then the study on the formation and degradation of passive films is reviewed. The mechanisms by which the alloying elements and microstructure affect the pitting corrosion are summarized. Finally, the academic progress of EAC is reviewed. The main conclusions are as follows.

(1) Among the reported failures, pitting corrosion and chloride-induced stress corrosion cracking are the main causes. Sulfide stress cracking, Hydrogen-induced stress cracking, MIC, selective corrosion and crevice corrosion are other failure causes. Therefore, academic studies should focus on the causes of such failures.

(2) The evolution of passive films after immersion in water can be roughly divided into three-stage, namely, the nucleation, rapid growth, and stable growth stages. The rupture process of the passive film is a continuous metal oxidation process rather than a sudden rupture. The film structure and composition

change simultaneously during the breakdown process.

(3) The film structure and film thickness of ferrite and austenite are very similar, whereas the chemical composition differs. Environment variables hardly change the double-layer structure of the passive film, but they change the overall thickness, oxide ratio, and defect concentration.

(4) The influence mechanisms of the alloying elements on pitting corrosion are summarized as the stabilization, ineffective, soluble precipitates, soluble inclusions, insoluble inclusions, and wrapping mechanisms. When the state of existence of the same alloying element changes, the influence mechanism varies.

(5) In the chloride-containing environment, ferrite is more prone to pitting corrosion than austenite. However, reversion of the pitting corrosion resistance occurs when a sufficiently large deformation is applied to duplex stainless steel. This is attributed to the greater number of defects generated in austenite.

(6) Three theories can be used to interpret the pitting corrosion mechanism of precipitants, namely (1) the Cr-depletion theory suggests that Cr-depleted zones surrounding precipitates cause pitting corrosion; (2) the microgalvanic theory proposes that the microgalvanic effect between Cr-enriched phase and Cr-depleted phase causes pitting corrosion; and (3) the high-stress field theory suggests that the high-stress field around the precipitates causes pitting corrosion.

(7) In chloride-induced stress corrosion cracking, chloride-induced cracks always initiate at corrosion pits and blunt upon contact with the austenite phase. In hydrogen-induced stress cracking, phase boundaries are not only strong hydrogen traps but also fast hydrogen diffusion pathways. The occurrence of sulfide stress cracking is closely related to the acidification effect of sulfide.

PROSPECTS

Owing to its high corrosion resistance, low economic cost, and good mechanical properties, duplex stainless steel is an ideal material for constructing future industrial societies. However, research on the corrosion of duplex stainless steel is still lacking. This review proposes important scientific issues and promising research directions in recent years.

(1) Studies on passive film formation are still lacking. The difference between the two phases at the micro-nanoscale and the longitudinal growth process of the passivation film from the cross-sectional perspective is still unclear. The effect of the cathodic potential on the passive film is still unclear. Therefore, it is necessary to use *in situ* scanning tunneling microscopy, high-resolution transmission microscopy, and theoretical model calculations to further explore this. Researchers need to pay more attention to the diffusion of elements along the phase boundaries.

(2) Studies on the nucleation and repassivation process of metastable pitting and the initiation process of submerged pitting corrosion are still lacking. Therefore, it is necessary to use *in situ* scanning tunneling microscopy and neutron scattering technology to study this. It is also necessary to perform quasi-*in situ* experiments, such as SKPFM and GIXRD, to understand these phenomena.

(3) The detailed mechanism of alloying elements to improve pitting corrosion still needs to be clarified because the alloying elements may play different roles in different stages of pitting corrosion. The coupling

law of more than two elements in pitting corrosion still needs to be explored. Therefore, it is necessary to use electrochemical corrosion combined with a pitting corrosion model to study this.

(4) Studies on the EAC of duplex stainless steels are not sufficient compared to the proportion of failures it has caused. The apparent regularity and microstructural mechanism of alloying elements on EAC are still unclear. Therefore, materials computing, metallurgy and electrochemistry should be used to study this and propose theoretical models.

(5) Duplex stainless steels are increasingly being used in a variety of applications. Therefore, it is necessary to study their corrosion behavior and mechanisms in more practical applications. Based on this, new types of corrosion-resistant, economical and high-strength duplex stainless steels should be developed.

DECLARATIONS

Authors' contributions

Made substantial contributions to the conception and design of the study and performed data acquisition, data analysis and interpretation: Liu M
Provided administrative and technical support: Du C, Liu Z, Li X, Wang L
Performed data acquisition: Zhong R, Cheng X, Ao J, Duan T, Zhu Y

Availability of data and materials

Not applicable.

Financial support and sponsorship

None.

Conflicts of interest

All authors declared that there are no conflicts of interest.

Ethical approval and consent to participate

Not applicable.

Consent for publication

Not applicable.

REFERENCES

1. Cobb HM. The history of stainless steel. ASM International; 2010. DOI
2. Silva B, Salvio F, Santos DD. Hydrogen induced stress cracking in UNS S32750 super duplex stainless steel tube weld joint. *Int J Hydrog Energy* 2015;40:17091-101. DOI
3. Colombo A, Trasatti S. Corrosion of an UNS S31803 distillation column for acetic acid recovery. *Eng Fail Anal* 2015;55:317-26. DOI
4. Chandra K, Singh A, Kain V, Kumar N. Sulphide stress cracking of a valve stem of duplex stainless steel. *Eng Fail Anal* 2018;94:41-6. DOI
5. Atxaga G, Irisarri A. Study of the failure of a duplex stainless steel valve. *Eng Fail Anal* 2009;16:1412-9. DOI
6. Wang H, Yang Y, Yang Z, Xu Z, Chai Y, Zhang Z. Corrosion failure analysis of duplex stainless steel in marine environment. *Int J Electrochem Sci* 2022;17:2. DOI
7. Liu W. Rapid MIC attack on 2205 duplex stainless steel pipe in a yacht. *Eng Fail Anal* 2014;42:109-20. DOI
8. Corleto CR, Argade GR. Failure analysis of dissimilar weld in heat exchanger. *Eng Fail Anal* 2017;9:27-34. DOI

9. Jebaraj A, Ajaykumar L, Deepak CR, Aditya KV. Weldability, machinability and surfacing of commercial duplex stainless steel AISI2205 for marine applications - a recent review. *J Adv Res* 2017;8:183-99. DOI PubMed PMC
10. Gowthaman P, Jeyakumar S, Saravanan B. Machinability and tool wear mechanism of duplex stainless steel - a review. *Mater Today Proc* 2020;26:1423-9. DOI
11. Westin EM. Hot cracking in duplex stainless steel weldments - a review. *Weld World* 2022;66:1483-99. DOI
12. Zhang D, Liu A, Yin B, Wen P. Additive manufacturing of duplex stainless steels - a critical review. *J Manuf Process* 2022;73:496-517. DOI
13. Verma J, Taiwade RV. Effect of welding processes and conditions on the microstructure, mechanical properties and corrosion resistance of duplex stainless steel weldments-a review. *J Manuf Process* 2017;25:134-52. DOI
14. Fan Y, Liu T, Xin L, Han Y, Lu Y, Shoji T. Thermal aging behaviors of duplex stainless steels used in nuclear power plant: a review. *J Nucl Mater* 2021;544:152693. DOI
15. Farias Azevedo CR, Boschetti Pereira H, Wolynec S, Padilha AF. An overview of the recurrent failures of duplex stainless steels. *Eng Fail Anal* 2019;97:161-88. DOI
16. Saithala JR, Kharusi A, Ghafri M, Nabhani T, Kulkarni M, Behlani N. After 30 years of duplex stainless steel experience in oil & gas-do we still face challenges? In: AMPP Annual Conference + Expo, San Antonio, TX, USA; 2022. Available from: https://onepetro.org/amppcorr/proceedings-abstract/AMPP22/4-AMPP22/D041S042R006/488731 [Last accessed on 11 April 2023].
17. Cassagne T, Embrittlement F. A review on hydrogen embrittlement of duplex stainless steels. Available from: https://onepetro.org/NACECORR/proceedings-abstract/CORR05/All-CORR05/NACE-05098/115159 [Last accessed on 11 April 2023].
18. Elhoud A, Renton N, Deans W. Hydrogen embrittlement of super duplex stainless steel in acid solution. *Int J Hydrog Energy* 2010;35:6455-64. DOI
19. Pan J. Studying the passivity and breakdown of duplex stainless steels at micrometer and nanometer scales - the influence of microstructure. *Front Mater* 2020;7:133. DOI
20. Han Y, Liu Z, Wu C, et al. A short review on the role of alloying elements in duplex stainless steels. *Tungsten* 2022:00168. DOI
21. Ha H, Lee T, Lee C, Yoon H. Understanding the relation between pitting corrosion resistance and phase fraction of S32101 duplex stainless steel. *Corros Sci* 2019;149:226-35. DOI
22. Ha H, Jang M, Lee T, Moon J. Interpretation of the relation between ferrite fraction and pitting corrosion resistance of commercial 2205 duplex stainless steel. *Corros Sci* 2014;89:154-62. DOI
23. Ha H, Jang M, Lee T, Moon J. Understanding the relation between phase fraction and pitting corrosion resistance of UNS S32750 stainless steel. *Mater Charact* 2015;106:338-45. DOI
24. Yao J, Macdonald DD, Dong C. Passive film on 2205 duplex stainless steel studied by photo-electrochemistry and ARXPS methods. *Corros Sci* 2019;146:221-32. DOI
25. Yao J, Qi Z, Dong C. Real-time evolution and characterization of passive films on individual ferrite and austenite phases of duplex stainless steel. *Electrochem Commun* 2022;137:107265. DOI
26. Ma L, Wiame F, Maurice V, Marcus P. Origin of nanoscale heterogeneity in the surface oxide film protecting stainless steel against corrosion. *NPJ Mater Degrad* 2019;3:1-9. DOI
27. Ma L, Wiame F, Maurice V, Marcus P. Stainless steel surface structure and initial oxidation at nanometric and atomic scales. *Appl Surf Sci* 2019;494:8-12. DOI
28. Örnek C, Långberg M, Evertsson J, et al. Influence of surface strain on passive film formation of duplex stainless steel and its degradation in corrosive environment. *J Electrochem Soc* 2019;166:C3071-80. DOI
29. Långberg M, Örnek C, Zhang F, et al. Characterization of native oxide and passive film on austenite/ferrite phases of duplex stainless steel using synchrotron HAXPEEM. *J Electrochem Soc* 2019;166:C3336-40. DOI
30. Rahimi E, Kosari A, Hosseinpour S, Davoodi A, Zandbergen H, Mol JM. Characterization of the passive layer on ferrite and austenite phases of super duplex stainless steel. *Appl Surf Sci* 2019;496:143634. DOI
31. Vignal V, Krawiec H, Heintz O, Mainy D. Passive properties of lean duplex stainless steels after long-term ageing in air studied using EBSD, AES, XPS and local electrochemical impedance spectroscopy. *Corros Sci* 2013;67:109-17. DOI
32. Gardin E, Zanna S, Seyeux A, Allion-maurer A, Marcus P. Comparative study of the surface oxide films on lean duplex and corresponding single phase stainless steels by XPS and ToF-SIMS. *Corros Sci* 2018;143:403-13. DOI
33. Gardin E, Zanna S, Seyeux A, Allion-maurer A, Marcus P. XPS and ToF-SIMS characterization of the surface oxides on lean duplex stainless steel - Global and local approaches. *Corros Sci* 2019;155:121-33. DOI
34. Liu H, Sun J, Qian J, et al. Revealing the temperature effects on the corrosion behaviour of 2205 duplex stainless steel from passivation to activation in a CO_2-containing geothermal environment. *Corros Sci* 2021;187:109495. DOI
35. Cui Z, Chen S, Dou Y, et al. Passivation behavior and surface chemistry of 2507 super duplex stainless steel in artificial seawater: influence of dissolved oxygen and pH. *Corros Sci* 2019;150:218-34. DOI
36. Cui Z, Wang L, Ni H, et al. Influence of temperature on the electrochemical and passivation behavior of 2507 super duplex stainless steel in simulated desulfurized flue gas condensates. *Corros Sci* 2017;118:31-48. DOI
37. Kan B, Wu W, Yang Z, Zhang X, Li J. Effects of hydrostatic pressure and pH on the corrosion behavior of 2205 duplex stainless steel. *J Electroanal Chem* 2021;886:115134. DOI
38. Wang L, Dou Y, Han S, Wu J, Cui Z. Influence of sulfide on the passivation behavior and surface chemistry of 2507 super duplex stainless steel in acidified artificial seawater. *Appl Surf Sci* 2020;504:144340. DOI

39. Yao J, Li N, Grothe H, Qi Z, Dong C. Determination of the hydrogen effects on the passive film and the micro-structure at the surface of 2205 duplex stainless steel. *Appl Surf Sci* 2021;554:149597. DOI
40. Guo LQ, Qin SX, Yang BJ, Liang D, Qiao LJ. Effect of hydrogen on semiconductive properties of passive film on ferrite and austenite phases in a duplex stainless steel. *Sci Rep* 2017;7:3317. DOI PubMed PMC
41. Chen L, Liu W, Dong B, et al. Insight into electrochemical passivation behavior and surface chemistry of 2205 duplex stainless steel: effect of tensile elastic stress. *Corros Sci* 2021;193:109903. DOI
42. Lv J, Guo W, Liang T. The effect of pre-deformation on corrosion resistance of the passive film formed on 2205 duplex stainless steel. *J Alloys Compd* 2016;686:176-83. DOI
43. Örnek C, Långberg M, Evertsson J, et al. In-situ synchrotron GIXRD study of passive film evolution on duplex stainless steel in corrosive environment. *Corros Sci* 2018;141:18-21. DOI
44. Långberg M, Örnek C, Evertsson J, et al. Redefining passivity breakdown of super duplex stainless steel by electrochemical operando synchrotron near surface X-ray analyses. *NPJ Mater Degrad* 2019;3:1-11. DOI
45. Ha HY, Lee CH, Lee TH, Kim S. Effects of nitrogen and tensile direction on stress corrosion cracking susceptibility of Ni-free FeCrMnC-based duplex stainless steels. *Materials* 2017;10:294. DOI PubMed PMC
46. Yan Z. Effects of Ni, Mn and N on microstructure and properties of 2507 super duplex stainless steel (In Chinese). In Harbin University of Science and Technology; 2014.
47. Baba H, Kodama T, Katada Y. Role of nitrogen on the corrosion behavior of austenitic stainless steels. *Corros Sci* 2002;44:2393-407. DOI
48. Merello R, Botana F, Botella J, Matres M, Marcos M. Influence of chemical composition on the pitting corrosion resistance of non-standard low-Ni high-Mn-N duplex stainless steels. *Corros Sci* 2003;45:909-21. DOI
49. An L, Cao J, Wu L, Mao H, Yang Y. Effects of Mo and Mn on pitting behavior of duplex stainless steel. *J Iron Steel Res Int* 2016;23:1333-41. DOI
50. Sun Y, Tan X, Lei L, Li J, Jiang Y. Revisiting the effect of molybdenum on pitting resistance of stainless steels. *Tungsten* 2021;3:329-37. DOI
51. Tian H, Cheng X, Wang Y, Dong C, Li X. Effect of Mo on interaction between α/γ phases of duplex stainless steel. *Electrochimica Acta* 2018;267:255-68. DOI
52. Kim JS, Xiang PJ, Kim KY. Effect of tungsten and nickel addition on the repassivation behavior of stainless steel. *Corros Sci* 2005;61:174-83. DOI
53. Potgieter J, Olubambi P, Cornish L, Machio C, Sherif EM. Influence of nickel additions on the corrosion behaviour of low nitrogen 22% Cr series duplex stainless steels. *Corros Sci* 2008;50:2572-9. DOI
54. Muthupandi V, Bala Srinivasan P, Shankar V, Seshadri S, Sundaresan S. Effect of nickel and nitrogen addition on the microstructure and mechanical properties of power beam processed duplex stainless steel (UNS 31803) weld metals. *Mater Lett* 2005;59:2305-9. DOI
55. Torres C, Hazarabedian MS, Quadir Z, Johnsen R, Iannuzzi M. The Role of tungsten on the phase transformation kinetics and its correlation with the localized corrosion resistance of 25Cr super duplex stainless steels. *J Electrochem Soc* 2020;167:081510. DOI
56. Ji L. Effect of tungsten on microstructure and properties of super duplex stainless steel $00Cr_{25}Ni_7Mo_{3.5}WCuN$ (In Chinese). In: Kunming University of Science and Technology; 2011.
57. Ran Q, Li J, Xu Y, Xiao X, Yu H, Jiang L. Novel Cu-bearing economical 21Cr duplex stainless steels. *Mater Des* 2013;46:758-65. DOI
58. Zhao Y, Liu X, Li X, Wang Y, Zhang W, Liu Z. Pitting corrosion behavior in novel Mn-N alloyed lean duplex stainless steel containing Cu. *J Mater Sci* 2018;53:824-36. DOI
59. Li P, Zhao Y, Liu Y, et al. Effect of Cu addition to 2205 duplex stainless steel on the resistance against pitting corrosion by the pseudomonas aeruginosa biofilm. *J Mater Sci Technol* 2017;33:723-7. DOI
60. Fuertes N, Pettersson R. Review-passive film properties and electrochemical response of different phases in a Cu-alloyed stainless steel after long term heat treatment. *J Electrochem Soc* 2016;163:C377-85. DOI
61. Fredriksson W, Edström K, Olsson C. XPS analysis of manganese in stainless steel passive films on 1.4432 and the lean duplex 1.4162. *Corros Sci* 2010;52:2505-10. DOI
62. Jang Y, Kim S, Lee J. Effect of different mo contents on tensile and corrosion behaviors of CD4MCU cast duplex stainless steels. *Metall Mat Trans A* 2005;36:1229-36. DOI
63. Li J, Xu Y, Xiao X, Zhao J, Jiang L, Hu J. A new resource-saving, high manganese and nitrogen super duplex stainless steel 25Cr-2Ni-3Mo-*x*Mn-N. *Mater Sci Eng A* 2009;527:245-51. DOI
64. Feng Z, Yang Y, Wang J. Effect of Mn addition on the precipitation and corrosion behaviour of 22% Cr economical duplex stainless steel after isothermal aging at 800 °C. *J Alloys Compd* 2017;699:334-44. DOI
65. Zhang J, Hu X, Chou K. Effects of Ti addition on microstructure and the associated corrosion behavior of a 22Cr-5Ni duplex stainless steel. *Mater Corros* 2021;72:1201-14. DOI
66. Li H. Dressing inclusions with "Niobium Armor": a new approach to improve the corrosion resistance of duplex stainless steels using niobium microalloying (In Chinese). In The 11th National Conference on Corrosion and Protection; 2021. DOI
67. Eleonora B, Raghuveer G, Karin A, Guocai C, Christina H, Siriki R. New duplex stainless steel 2018. (EP 3631031A1).
68. Junichiro K, Natsuki N, Nii H, Sato T. Duplex stainless steel material and duplex stainless steel tube; 2015. (EP 2947169A1).

69. Kawamori M, Kinugasa J, Fukuta Y, et al. Pitting corrosion resistance of Ta-bearing duplex stainless steel. *Mater Trans* 2021;62:1359-67. DOI
70. Meng Q, La P, Yao L, Zhang P, Wei Y, Guo X. Effect of Al on microstructure and properties of hot-rolled 2205 dual stainless steel. *Adv Mater Sci Eng* 2016;2016:1-8. DOI
71. Huang W, Chen C, Chou Y, Lin D, Yang S. Pitting corrosion behavior of silver-containing 2205 duplex stainless steel as secondary austenitic phase existed. *Mater Trans* 2013;54:553-60. DOI
72. Jeon S, Kim S, Lee J, Lee I, Park Y. Effects of sulfur addition on the formation of inclusions and the corrosion behavior of super duplex stainless steels in chloride solutions of different pH. *Mater Trans* 2012;53:1617-26. DOI
73. Kim SM, Kim JS, Kim KT, Park K, Lee CS. Effect of Ce addition on secondary phase transformation and mechanical properties of 27Cr-7Ni hyper duplex stainless steels. *Mater Sci Eng A* 2013;573:27-36. DOI
74. Kim S, Jeon S, Lee I, Park Y. Effects of rare earth metals addition on the resistance to pitting corrosion of super duplex stainless steel - part 1. *Corros Sci* 2010;52:1897-904. DOI
75. Shinji T, Yusuke O, Hiroshi U, Haruhiko K. Duplex stainless steel, duplex stainless steel slab, and duplex stainless steel material; 2014. (US 2014255244A1).
76. Potgieter JH, Ellis P, Bennekom AV. Investigation of the active dissolution behaviour of a 22% chromium duplex stainless steel with small ruthenium additions in sulphuric acid. *ISIJ Int* 1995;35:197-202. DOI
77. Örnek C, Engelberg D. SKPFM measured volta potential correlated with strain localisation in microstructure to understand corrosion susceptibility of cold-rolled grade 2205 duplex stainless steel. *Corros Sci* 2015;99:164-71. DOI
78. Mondal R, Bonagani SK, Lodh A, et al. Relating general and phase specific corrosion in a super duplex stainless steel with phase specific microstructure evolution. *Corrosion* 2019;75:1315-26. DOI
79. Tsai W, Chen J. Galvanic corrosion between the constituent phases in duplex stainless steel. *Corros Sci* 2007;49:3659-68. DOI
80. Jimei X. Metallography of stainless steel (In Chinese). Beijing: Metallurgical Industry Press; 1983. p. 122-3.
81. Cheng X, Wang Y, Dong C, Li X. The beneficial galvanic effect of the constituent phases in 2205 duplex stainless steel on the passive films formed in a 3.5% NaCl solution. *Corros Sci* 2018;134:122-30. DOI
82. Luo H, Wang X, Dong C, Xiao K, Li X. Effect of cold deformation on the corrosion behaviour of UNS S31803 duplex stainless steel in simulated concrete pore solution. *Corros Sci* 2017;124:178-92. DOI
83. Fréchard S, Martin F, Clément C, Cousty J. AFM and EBSD combined studies of plastic deformation in a duplex stainless steel. *Mater Sci Eng A* 2006;418:312-9. DOI
84. Frankel GS, Li T, Scully JR. Perspective-localized corrosion: passive film breakdown *vs.* pit growth stability. *J Electrochem Soc* 2017;164:C180-1. DOI
85. Li T, Scully JR, Frankel GS. Localized corrosion: passive film breakdown *vs.* pit growth stability: part V. Validation of a new framework for pit growth stability using one-dimensional artificial pit electrodes. *J Electrochem Soc* 2019;166:C3341-54. DOI
86. Li M, Seyeux A, Wiame F, Marcus P, Światowska J. Insights on the Al-Cu-Fe-Mn intermetallic particles induced pitting corrosion of Al-Cu-Li alloy. *Corros Sci* 2020;176:109040. DOI
87. Jeon S, Kim H, Park Y. Effects of inclusions on the precipitation of chi phases and intergranular corrosion resistance of hyper duplex stainless steel. *Corros Sci* 2014;87:1-5. DOI
88. Zhang Z, Jing H, Xu L, Han Y, Zhao L. The influence of microstructural evolution on selective corrosion in duplex stainless steel flux-cored arc welded joints. *Corros Sci* 2017;120:194-210. DOI
89. Santos DCD, Magnabosco R, de Moura-neto C. Influence of sigma phase formation on pitting corrosion of an aged UNS S31803 duplex stainless steel. *Corrosion* 2013;69:900-11. DOI
90. Jinlong L, Tongxiang L, Limin D, Chen W. Influence of sensitization on microstructure and passive property of AISI 2205 duplex stainless steel. *Corros Sci* 2016;104:144-51. DOI
91. Zhang Z, Zhao H, Zhang H, et al. Effect of isothermal aging on the pitting corrosion resistance of UNS S82441 duplex stainless steel based on electrochemical detection. *Corros Sci* 2015;93:120-5. DOI
92. Hong J, Han D, Tan H, Li J, Jiang Y. Evaluation of aged duplex stainless steel UNS S32750 susceptibility to intergranular corrosion by optimized double loop electrochemical potentiokinetic reactivation method. *Corros Sci* 2013;68:249-55. DOI
93. Melo EB, Magnabosco R. Evaluation of microstructural effects on the degree of sensitization (DOS) of a UNS S31803 duplex stainless steel aged at 475 °C. *Corrosion* 2015;71:1490-9. DOI
94. Silva R, Vacchi G, Kugelmeier C, et al. New insights into the hardening and pitting corrosion mechanisms of thermally aged duplex stainless steel at 475 °C: a comparative study between 2205 and 2101 steels. *J Mater Sci Technol* 2022;98:123-35. DOI
95. Silva R, Kugelmeier C, Vacchi G, et al. A comprehensive study of the pitting corrosion mechanism of lean duplex stainless steel grade 2404 aged at 475 °C. *Corros Sci* 2021;191:109738. DOI
96. Chen Y, Yang B, Zhou Y, Wu Y, Zhu H. Evaluation of pitting corrosion in duplex stainless steel $Fe_{20}Cr_9Ni$ for nuclear power application. *Acta Mater* 2020;197:172-83. DOI
97. Zhang B, Ma X. A review-Pitting corrosion initiation investigated by TEM. *J Mater Sci Technol* 2019;35:1455-65. DOI
98. Pan S, Dong S, Xu M. Electrochemical origin for mitigated pitting initiation in AA7075 alloy with TiB2 nanoparticles. *Appl Surf Sci* 2022;601:154275. DOI
99. Raja V, Shoji T. Stress corrosion cracking: theory and practice. Elsevier; 2011. Available from: https://www.researchgate.net/publication/297926155_Stress_corrosion_cracking_Theory_and_practice [Last accessed on 15 Apr 2023].

100. Scully JC. Mechanism of dissolution-controlled cracking. *Metal Sci* 1978;12:290-300. DOI
101. Liu H. A unified model of environment-assisted cracking. *Acta Mater* 2008;56:4339-48. DOI
102. Mcmahon C. Hydrogen-induced intergranular fracture of steels. *Eng Fract Mech* 2001;68:773-88. DOI
103. Birnbaum H, Robertson I, Sofronis P, Teter D. Mechanisms of hydrogen related fracture-a review. In: Second International Conference on Corrosion-Deformation Interactions; 1996. pp. 172-95. Available from: https://www.researchgate.net/publication/287494691_Mechanisms_of_hydrogen_related_fracture_-_a_review_in_T_Magnin_Ed [Last accessed on 15 Apr 2023].
104. Barnes A, Senior NA, Newman RC. Film-induced cleavage of Ag-Au alloys. *Metall Mat Trans A* 2009;40:58-68. DOI
105. Eguchi K, Burnett TL, Engelberg DL. X-ray tomographic observation of environmental assisted cracking in heat-treated lean duplex stainless steel. *Corros Sci* 2021;184:109363. DOI
106. Zanotto F, Grassi V, Balbo A, Monticelli C, Zucchi F. Stress corrosion cracking of LDX 2101® duplex stainless steel in chloride solutions in the presence of thiosulphate. *Corros Sci* 2014;80:205-12. DOI
107. Wu W, Zhang X, Li W, et al. Effect of hydrogen trapping on hydrogen permeation in a 2205 duplex stainless steel: role of austenite-ferrite interface. *Corros Sci* 2022;202:110332. DOI
108. Zucchi F, Grassi V, Monticelli C, Trabanelli G. Hydrogen embrittlement of duplex stainless steel under cathodic protection in acidic artificial sea water in the presence of sulphide ions. *Corros Sci* 2006;48:522-30. DOI
109. Klyk-spyra K, Sozańska M. Quantitative fractography of 2205 duplex stainless steel after a sulfide stress cracking test. *Mater Charact* 2006;56:384-8. DOI
110. Laitinen A, Hänninen H. Chloride-induced stress corrosion cracking of powder metallurgy duplex stainless steels. *Corrosion* 1996;52:295-306. DOI
111. Wu W, Liu Z, Hu S, Li X, Du C. Effect of pH and hydrogen on the stress corrosion cracking behavior of duplex stainless steel in marine atmosphere environment. *Ocean Eng* 2017;146:311-23. DOI
112. Raman RS, Siew W. Role of nitrite addition in chloride stress corrosion cracking of a super duplex stainless steel. *Corros Sci* 2010;52:113-7. DOI
113. Rajaguru J, Arunachalam N. Investigation on machining induced surface and subsurface modifications on the stress corrosion crack growth behaviour of super duplex stainless steel. *Corros Sci* 2018;141:230-42. DOI
114. Wickström L, Mingard K, Hinds G, Turnbull A. Microcrack clustering in stress corrosion cracking of 22Cr and 25Cr duplex stainless steels. *Corros Sci* 2016;109:86-93. DOI
115. Örnek C, Zhong X, Engelberg DL. Low-temperature environmentally assisted cracking of grade 2205 duplex stainless steel beneath a $MgCl_2$:$FeCl_3$ salt droplet. *Corrosion* 2016;72:384-99. DOI
116. Sofia Hazarabedian M, Viereckl A, Quadir Z, et al. Hydrogen-induced stress cracking of swaged super duplex stainless steel subsea components. *Corrosion* 2019;75:824-38. DOI
117. Maeda MY, Koyama M, Nishimura H, Cintho OM, Akiyama E. Hydrogen-assisted damage evolution in nitrogen-doped duplex stainless steel. *Int J Hydrog Energy* 2021;46:2716-28. DOI
118. Liang X, Dodge M, Kabra S, Kelleher J, Lee T, Dong H. Effect of hydrogen charging on dislocation multiplication in pre-strained super duplex stainless steel. *Scr Mater* 2018;143:20-4. DOI
119. Örnek C, Larsson A, Harlow GS, et al. Metastable precursor structures in hydrogen-infused super duplex stainless steel microstructure - an operando diffraction experiment. *Corros Sci* 2020;176:109021. DOI
120. Claeys L, Depover T, De Graeve I, Verbeken K. First observation by EBSD of martensitic transformations due to hydrogen presence during straining of duplex stainless steel. *Mater Charact* 2019;156:109843. DOI
121. Barnoush A, Zamanzade M, Vehoff H. Direct observation of hydrogen-enhanced plasticity in super duplex stainless steel by means of *in situ* electrochemical methods. *Scr Mater* 2010;62:242-5. DOI
122. Örnek C, Larsson A, Harlow GS, et al. Time-resolved grazing-incidence X-ray diffraction measurement to understand the effect of hydrogen on surface strain development in super duplex stainless steel. *Scr Mater* 2020;187:63-7. DOI
123. Tong H, Sun Y, Su Y, Pang X, Gao K. Investigation on hydrogen-induced cracking behavior of 2205 duplex stainless steel used for marine structure (In Chinese). *J Chin Soc Corros Prot* 2019;39:130-7. DOI
124. El-Sherik MA. Trends in oil and gas corrosion research and technologies; 2017. pp. 271-92. DOI
125. Saithala JR, Sudhakar M, Ubhi HS, Atkinson JD. Environmental-assisted cracking behaviour of sigmatied super duplex stainless steel in oil field production brine. 2012. DOI